

University of Windsor Scholarship at UWindsor

Electronic Theses and Dissertations

1973

Mass transfer with chemical reaction in gas liquid cocurrent vertical flow.

Fernando J. Di Pierdomenico
University of Windsor

Follow this and additional works at: <http://scholar.uwindsor.ca/etd>

Recommended Citation

Di Pierdomenico, Fernando J., "Mass transfer with chemical reaction in gas liquid cocurrent vertical flow." (1973). *Electronic Theses and Dissertations*. Paper 2671.

This online database contains the full-text of PhD dissertations and Masters' theses of University of Windsor students from 1954 forward. These documents are made available for personal study and research purposes only, in accordance with the Canadian Copyright Act and the Creative Commons license—CC BY-NC-ND (Attribution, Non-Commercial, No Derivative Works). Under this license, works must always be attributed to the copyright holder (original author), cannot be used for any commercial purposes, and may not be altered. Any other use would require the permission of the copyright holder. Students may inquire about withdrawing their dissertation and/or thesis from this database. For additional inquiries, please contact the repository administrator via email (scholarship@uwindsor.ca) or by telephone at 519-253-3000ext. 3208.

MASS TRANSFER WITH CHEMICAL REACTION IN GAS LIQUID
COCURRENT VERTICAL FLOW

A Thesis

Submitted to the Faculty of Graduate Studies Through the
Department of Chemical Engineering in Partial Fulfilment
of the Requirements for the Degree of
Master of Applied Science at the
University of Windsor

by

Fernando J. Di Pierdomenico

Windsor, Ontario
1973

© Fernando J. Di Pierdomenico 1973

437378

ABSTRACT

Measurements of overall mass transfer coefficients for the chemical absorption of carbon dioxide into monoethanolamine solutions have been made in slug and transition two-phase regimes in a 1/2-in. I.D. vertical tube. Effect of dimensionless gas and liquid velocities and monoethanolamine concentration on the overall mass transfer coefficient has been studied. A relatively new technique for obtaining gas free liquid samples from the test section was used and effective interfacial areas and gas film coefficients have been computed by making use of a technique proposed by Wales.

Pressure drop predictions were made using a method proposed by Powley. A regime constant was calculated and a plot of predicted pressure gradients against those measured indicate a very good accuracy of the proposed method. A new relation for liquid volume fraction as a function of the Lockhart-Martenelli parameters is suggested by the data.

The results for the mass transfer experiments agree in order of magnitude with those obtained by Weiland for a vertical packed tower. Contrary to the findings of Kahol, the mass transfer results contained in this study are influenced, to a large degree, by gravity.

ACKNOWLEDGEMENTS

The author wishes to express his sincere gratitude to Professor M.B. Powley and Mr. K. Petrunik for their guidance throughout this work. The author is also very thankful to Mr. R. A. Foster for his consideration while continuing his studies during his first working year in industry.

Special thanks go to my wife, Patricia, who has spent many hours in the laboratory with me and who has provided encouragement and assistance in completing the thesis.

The financial support for this work was provided by the National Research Council of Canada.

CONTENTS

	Page
ABSTRACT	111
ACKNOWLEDGEMENTS	iv
TABLE OF CONTENTS	v
LIST OF FIGURES	vii
LIST OF TABLES	viii
I. INTRODUCTION	1
II. LITERATURE REVIEW	4
III. THEORY	
A. The Reaction Between Carbon Dioxide and MEA	6
B. The Prediction of Mass Transfer Coefficients	7
C. The Overall Mass Transfer Coefficient and Determination of Interfacial Areas	11
D. Two-Phase Pressure Drop in Vertical Flow	12
E. Estimation of Physico-Chemical Parameters	13
IV. EXPERIMENTAL APPARATUS AND PROCEDURE	
A. Description of Apparatus	17
B. Pressure Measurements	20
C. Sampling Technique and Analysis	20
D. Experimental Procedure	23
V. EXPERIMENTAL RESULTS AND DISCUSSION	
A. Pressure Drop	25
B. Overall Mass Transfer Coefficient	28
C. Interfacial Areas	34
D. Individual Film Coefficients	34

E. Accuracy of Results	36
VI. CONCLUSIONS	39
NOMENCLATURE	40
REFERENCES	44
APPENDIX I Computer Program Listing and Output	46
APPENDIX II Analysis of Variance	51
APPENDIX III System Parameters	52
APPENDIX IV Calibration and Titration Curves	56
VITA AUCTORIS	60

FIGURES

<u>Figure</u>	<u>Page</u>
1. Flow Pattern Chart for Vertical Flow	3
2. Two-Film Concentration Profiles	9
3. Schematic Diagram of Experimental Set-up	18
4. Test Section Details	19
5. Pressure Measuring System	21
6. Gravity Separator Type Liquid Sampler	22
7. Comparison of Powley's Pressure Drop Model With Experimental Data	26
8. Lockhart-Martenelli Functions	27
9. Effect of Dimensionless Velocities on Overall Mass Transfer Coefficient for $b_0 = 0.171$	29
10. Effect of Dimensionless Velocities on Overall Mass Transfer Coefficient for $b_0 = 0.257$	30
11. Effect of Dimensionless Velocities on Interfacial Area	35
12. Effect of Dimensionless Velocities on the Gas Film Coefficient	37
13. Reaction Rate Constant	53
14. Ionization Data	54
15. Flooding Velocities for Air and Water	55
16. Calibration Curve for Carbon Dioxide Rotameter	57
17. Calibration Curve for Liquid Rotameter	58
18. Titration Curve for MEA	59

TABLES

<u>Table</u>	<u>Page</u>
1. Regression Coefficients	32
2. Analysis of Variance	51
3. Uncertainty Limits in Variables	38

I. INTRODUCTION

Mass transfer to two-phase flowing systems is a common occurrence in industrial absorbers and strippers. The desirability of such equipment is reflected by its efficiency (degree of separation) and process economics. Industrial use of a chemical absorbent usually depends on its recoverability. For this reason, monoethanolamine (hereafter referred to as MEA) has experienced widespread use in the absorption of carbon dioxide gas. The lack of design data; however, has limited its use in pipeline contactors.

Chemical absorption using MEA is a highly complex topic requiring extensive knowledge of thermodynamics, chemical kinetics, and two-phase hydrodynamics. The complete process may be described as diffusion of solute gas from the gas bulk through the liquid interface to the reaction site, the reaction of carbon dioxide with MEA, and the diffusion of reactant products into the bulk of the liquid. The measured resistance of each phase will indicate the suitability of the absorbent.

To obtain a model for the overall mass transfer coefficient based on the flow parameters and physico-chemical constants, carbon dioxide concentration has been limited to approximately 5% of the total gas flow. As a result, there will be negligible temperature change from one end of the column to the other. Thus, the volumetric coefficient for

mass transfer and interfacial areas may be calculated and compared to values characteristic of packed towers.

The advantages of pipeline reactors include low capital cost, high degree of agitation reflecting high transfer rates, ease of handling a wide cross-section of solutions including slurries and foam, and low maintenance cost. Among the disadvantages are included high pumping costs for the high flow rates and long reactor lengths for increased contact time.

The object of this study was primarily to measure the effects of concentration and fluid velocities on the overall volumetric mass transfer coefficient. Furthermore, through proper manipulation of the equations; effective interfacial areas for mass transfer and individual film resistances were also recorded. Of secondary importance was the prediction of two-phase pressure drop in vertical pipes.

The system of interest is CO_2 and Air - flowing cocurrently with a dilute aqueous solution of MEA in a vertical 1/2-in. I.D. tube. The regions under investigation include both slug and transition zones which are shown on the regime chart by Wallis (1) in Figure 1.

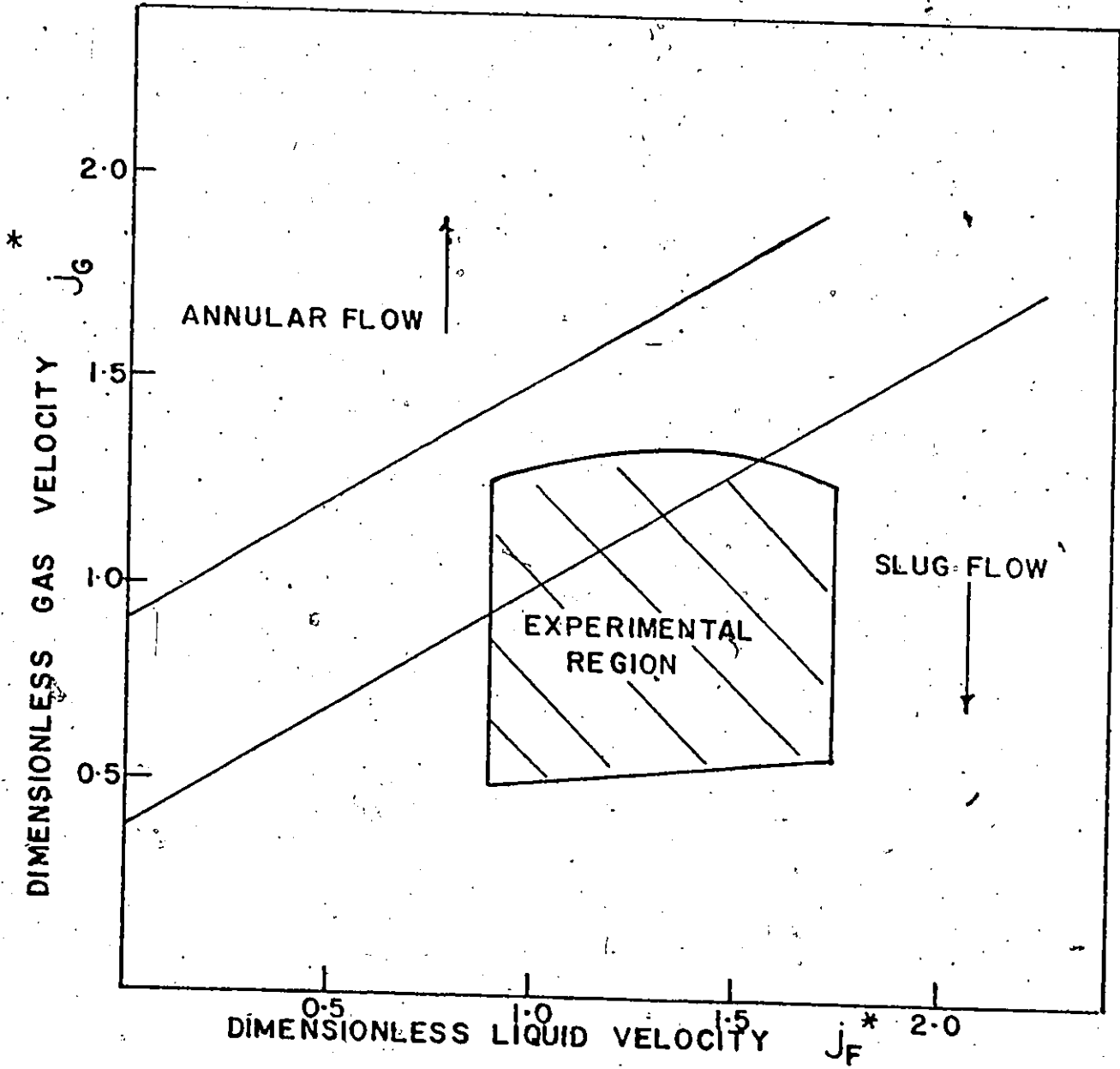


FIG.1 FLOW CHART FOR CO-CURRENT UP FLOW

II. PREVIOUS WORK

Many researchers have investigated the concept of mass transfer in two-phase flow. Most literature to date concentrates on packed towers and horizontal contactors.

Heuss et al. (2) have studied the absorption of ammonia in horizontal cocurrent gas-liquid froth flow in a 1 in. I.D. pipe. The ammonia absorption data indicated a gas-phase controlled system with both the gas and liquid coefficients showing increases in value as bubble diameter decreased.

Emmert and Pigford (3) conducted experiments on the absorption of carbon dioxide in aqueous solutions of MEA in a very short wetted wall column. The observed results indicate that with an increase in contact time the liquid coefficient decreases and further plots reveal negligible nonequilibrium at the interface indicating that the influence of the reaction rate is negligible. Brian et al. (4) have shown that the physical mass transfer coefficient is increased substantially by the carbon dioxide-MEA chemical absorption process. This is presumably due to interfacial turbulence which is driven by surface tension gradients. Van Heuven and Beek (5) have presented data for the physical absorption of carbon dioxide from a mixture of carbon dioxide-nitrogen into water by using gas lifts of 0.48 and 0.238 cm. I.D. and 0.5 and 1.0 m. long. The experiments were performed in the slug flow regime and results indicate a predominant liquid phase resistance.

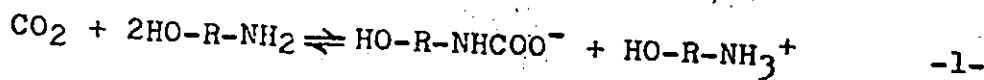
Kahol (6) has conducted chemical absorption experiments in a vertical two-phase system of carbon dioxide-air and sodium hydroxide solution. The overall volumetric coefficient was reported for a 1/2 in. I.D. plexiglass column. Interfacial areas and gas film coefficients were calculated by using techniques developed by Wales (7). Recent studies, carried out by Bradley and Andre (8), indicate the transient behaviour of CO₂ - MEA systems when subjected to step and pulse changes in feed rates. The experimental equipment consisted of 3 in. I.D. glass column 10 ft. long, packed to a height of 9.25 ft. with 3/8 in. x 3/8 in. x 1/16 in. glass Raschig rings. Liquid feed rate varied from 65.5 to 82.1 lb. mole/ft.² hr., and gas feed rate varied from 9.55 to 10.01 lb. mole/ft.² hr. Outlet composition response to positive and negative step forcing of feed gas concentration indicates onset of steady state after 4 to 5 min.

III. THEORY

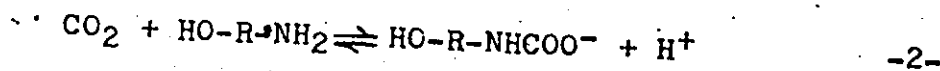
A. The Reaction Between Carbon Dioxide and MEA

Chemical absorption of carbon dioxide in aqueous solutions of MEA has been studied widely and the reaction mechanism for the chemical combination of CO₂ with MEA is well known (9). MEA is bifunctional; that is, the molecule has an -OH group on one end, which may react with CO₂ to form carbonic acid, and a -NH₂ group at the other end, which may react with CO₂ to form carbamic acid. The reaction with the hydroxyl group takes place in basic solution of pH greater than 11, but since the pH of uncarbonated MEA solution is less than 10, this reaction may be disregarded.

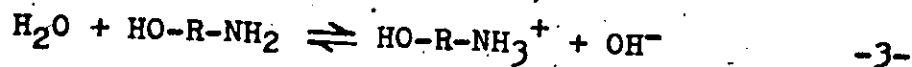
For carbonation ratios less than one-half, the overall chemical reaction between CO₂ and MEA in the liquid phase has been studied by Astartita (9) and by Dankwertz et al. (10). The overall reaction is represented in equation 1.



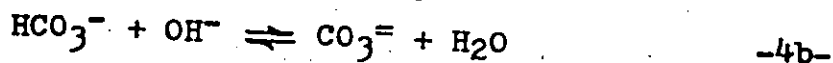
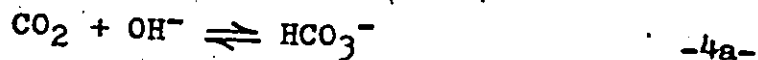
The reaction presumably occurs in two steps. First is the direct attack of CO₂ on the primary amine to form carbamic acid:



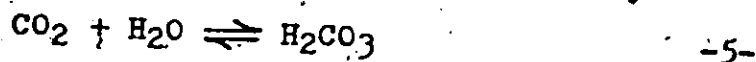
and second, the hydrolysis of the amine to form the ammonium ion.



The hydrolysis ion resulting from the hydrolysis reaction also reacts with CO_2 forming bicarbonate and carbonate ions.



Finally, carbonic acid is formed by the reaction of CO_2 with water.



According to Emmert and Pigford (3) the reaction involving the formation of the carbamate is most important in influencing the absorption rate. The hydrolysis of the amine, which involves only the transfer of a proton, occurs almost instantaneously and consequently is not rate controlling.

Pinsent et al. (11) describes the hydrolysis of CO_2 as a very slow reaction with a rate constant of 0.025 l./gm. mole sec. at 25° C.; therefore, having negligible effect on the absorption rate.

Emmert and Pigford (3) have found that at total equilibrium the formation of the carbonate is favoured and when this reaction is complete, the solution has a higher pH and a lower partial pressure of CO_2 .

B. The Prediction of Mass Transfer Coefficients

To describe the unidirectional movement of CO_2 from a

plane interface, the Navier-Stokes equations for mass transfer may be simplified to describe this steady state process of simultaneous diffusion accompanied by chemical reaction in a stagnant liquid. The mathematical equation is as follows:

$$D \frac{d^2 [CO_2]}{dx^2} = k [CO_2] [MEA] \quad -6-$$

where
D = diffusivity of CO₂ in the liquid phase
x = distance from the interface
k = reaction rate constant between CO₂ and MEA in the liquid phase.

The general form of the concentration profiles for equation 6 is shown in Figure 2a.

The assumption is now made that [MEA] is large enough so that reaction with CO₂ causes negligible change in its value. In effect, this implies a pseudo first order reaction; whereby, the [MEA] becomes constant. This situation is illustrated in Figure 2b. All dissolved gas reacts in the film and the reaction products are carried into the bulk of the liquid. The mathematical description and boundary conditions for the pseudo first order reaction are illustrated below:

$$D \frac{d^2 [CO_2]}{dx^2} = k' [CO_2] \quad -7-$$

where
and

$$k' = k [MEA]$$
$$[CO_2] = [CO_2]_e \quad \text{at } x = 0$$
$$[CO_2] = 0 \quad \text{at } x = \delta_L$$

FIG. 2a.

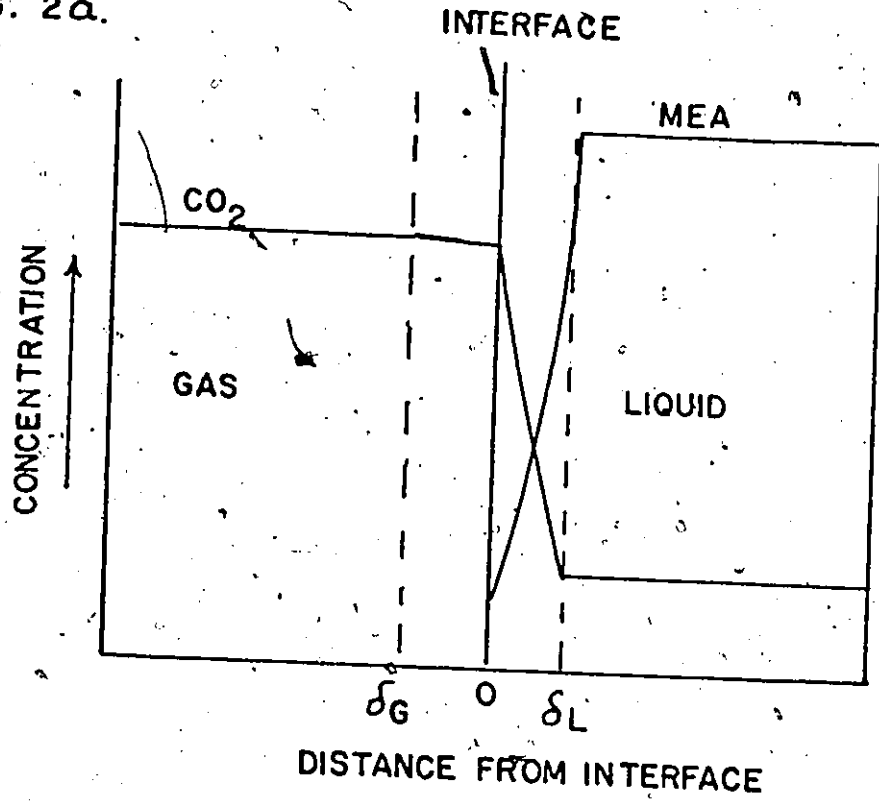


FIG. 2b.

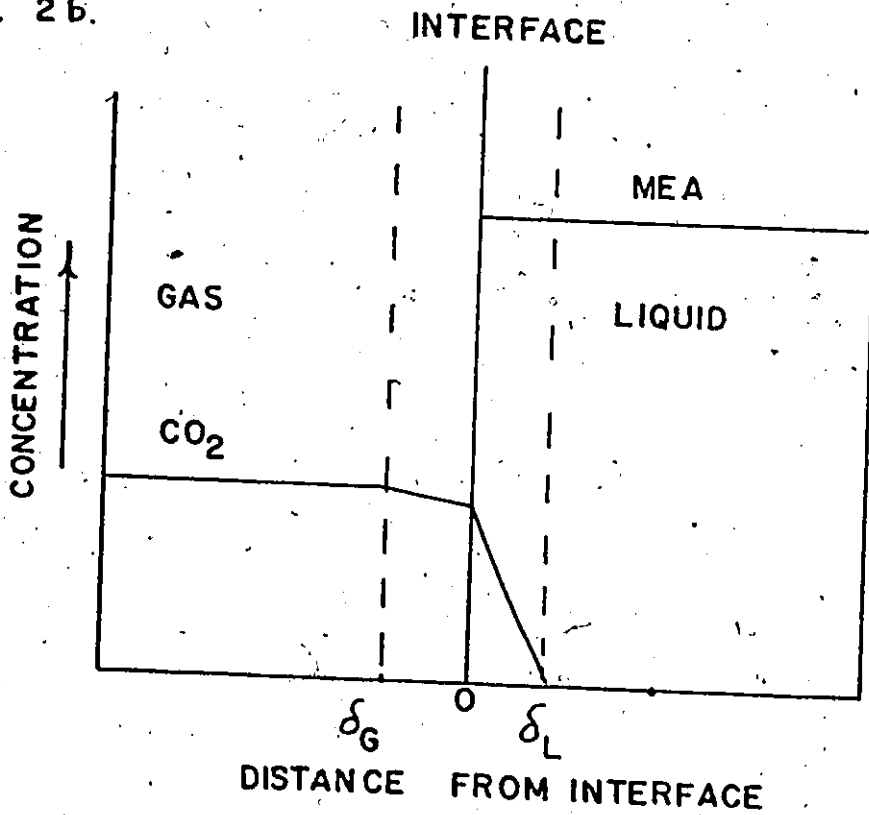


FIG. 2. CONCENTRATION PROFILES

The solution of equation 7 gives the concentration profile of unreacted CO_2 in the liquid film:

$$\frac{[\text{CO}_2]}{[\text{CO}_2]_e} = \exp(-x(k^*/D)^{1/2}) \quad -8-$$

The absorption rate is by definition:

$$N = D \left(\frac{d[\text{CO}_2]}{dx} \right) \Big|_{x=0} = [\text{CO}_2]_e (Dk^*)^{1/2} \quad -9-$$

where N = absorption rate per unit interfacial area. From equation 9 it follows that the liquid film mass transfer coefficient is:

$$k_L = (Dk^*)^{1/2} \quad -10-$$

From equation 10 it is evident that the absorption coefficient k_L is a function only of the physico-chemical parameters of the system.

Under the condition of absorption at low concentrations of CO_2 , Dankwertz (12) has proposed the following criteria for the gas undergoing a pseudo first order reaction:

$$(Dk^*)^{1/2}/k_L^0 \ll 1 + \frac{[\text{MEA}]}{Z[\text{CO}_2]_e} \quad -11-$$

where

k_L^0 = physical absorption liquid film coefficient

Z = the number of moles of reagent which reacts (stoichiometrically) with one mole of CO_2 .

Appendix I illustrates the validity of the criterion at points of interest in the column.

C. The Overall Mass Transfer Coefficient and Determination of Interfacial Areas

The two film theory has provided the concept of addition of individual film resistances which act in series. Equation 12 relates the individual transfer coefficients to the overall coefficient based on the gas side.

$$\frac{1}{K_G \cdot a} = \frac{1}{k_G \cdot a} + \frac{m}{k_L \cdot a} \quad -12-$$

where

m = slope of the equilibrium curve

a = effective interfacial area for mass transfer.

For dilute systems " m " may be replaced by Henry's Law Constant " H " as in equation 13.

$$\frac{1}{K_G \cdot a} = \frac{1}{k_G \cdot a} + \frac{H}{k_L \cdot a} \quad -13-$$

It is evident from equation 13 that by varying hydrodynamic and physico-chemical parameters, a plot of " $1/K_G \cdot a$ " vs. " H/k_L " may be made having a slope of " $1/a$ " and an intercept of " $1/k_G \cdot a$ ". Since the interfacial area is partially influenced by liquid viscosity and surface tension, it is assumed that these parameters do not effect the interfacial area as MEA changes. This assumption becomes valid, since the maximum change in concentration is approximately 0.1 moles/litre.

D. Two-Phase Pressure Drop in Vertical Flow

The pressure drop of a vertical two-phase system consists of three components: frictional loss, momentum change, and change in elevation.

$$(dp/dz)_T = (dp/dz)_F + (dp/dz)_M + (dp/dz)_E \quad -14-$$

For turbulent-turbulent flow, Powley's correlation adopts the concept of the Lockhart-Martenelli " X_{tt} " which is defined as the square root of the ratio of frictional pressure drop of the liquid flowing alone to that of the gas flowing alone.

$$X_{tt} = \left((dp/dz)_{LP} / (dp/dz)_{GP} \right)^{1/2} \quad -15-$$

The expression for the two-phase friction pressure drop in terms of the single phase friction pressure drop of the liquid flowing alone is:

$$(dp/dz)_{TPF} = (dp/dz)_{LP} \phi_{Ltt}^2 \quad -16-$$

and ϕ_{Ltt}^2 is an empirical function of X_{tt} .

$$\phi_{Ltt}^2 = 1 + \frac{1}{X_{tt}^2} + \frac{A}{X_{tt}} \left[\left(\frac{\rho_R}{\rho_G} \right)^{1/2} + \left(\frac{\rho_G}{\rho_F} \right)^{1/2} \right] \quad -17-$$

and A is a constant characteristic of the flow regime. For this system $A = 0.76$.

The relationship for liquid volume fraction in slug flow is given by Wallis (13) as:

$$R_{LS} = 1 - \frac{j_G^* (\rho_F / \rho_G)^{1/2}}{1.2(j_F^* + j_G^* (\rho_F / \rho_G)^{1/2}) + 0.345} \quad -18a-$$

where $j_G^* = v_G \rho_G^{1/2} (d_g(\rho_F - \rho_G))^{-1/2} \quad -18b-$

$$j_F^* = v_F \rho_F^{1/2} (d_g(\rho_F - \rho_G))^{-1/2} \quad -18c-$$

With equation 18a the elevation pressure drop may be calculated:

$$(dp/dz)_E = \rho_F R_{LS} + (1 - R_{LS}) \rho_G \quad -19-$$

With the assumption of homogeneous flow, momentum pressure drop can be evaluated by equation 20.

$$(dp/dz)_M = \frac{G^2 X}{1g_c \rho_{Gin}} \left(\frac{1 - P_{in}}{P_{out}} \right) \quad -20-$$

E. Estimation of Physico-Chemical Parameters

Because of the large numbers of parameters involved in calculating mass transfer coefficients, each parameter will be dealt with separately.

1. Density Data

The density of MEA solutions at low concentrations doesn't vary significantly from that of water. Therefore; for all practical purposes, the density of water at that temperature was taken from the "CRC Handbook of Physics and Chemistry" (14) and used in all calculations. The density of Air - CO₂ gas mixture was obtained by using the ideal gas law.

2. Viscosity Data

The viscosity of water at various temperatures was

taken from the "CRC Handbook of Physics and Chemistry" (14). Viscosity data for MEA solutions was obtained from the work of Thomas and Furzer (15).

3. Diffusion Data

To predict the diffusion coefficient of CO₂ in water the Wilke-Chang correlation (16) was used.

$$D = 7.4 \times 10^{-8} \frac{(\chi M)^{1/2} T}{\mu \bar{V}^{0.6}} \quad -21-$$

where

T = temperature in °K

\bar{V} = molecular volume of solute at the normal boiling point cm.³/gm. mole

χ = Association parameter equal to 2.6 for water.

M = molecular weight of solvent.

μ = viscosity of solution cp.

Predicted variations of reagent diffusivity with MEA concentration was obtained from the data of Thomas and Furzer (15). In describing the effect of amine concentration on the diffusivity of CO₂ in solution, it has been assumed that the diffusivity of CO₂ is affected to the same extent by amine concentration as is the amine diffusivity. This relationship has been discussed by Dankwertz and Sharma (17).

$$\frac{D_{CA}}{D_{CW}} = \frac{D_{AA}}{D_{AW}}$$

4. Physical Solubility of Carbon Dioxide in MEA Solutions

When considering gas absorption accompanied by chemical reaction it is not possible to measure the physical solubility of CO_2 . However, Astarita (9) has made use of the available data for electrolytic solution to infer the solubility in reactive media. Therefore, solubility of CO_2 in water containing various ions, may be corrected by the following equation:

$$\log_{10} \left(\frac{H_e}{H_e^0} \right) = hI \quad -23a-$$

$$h = h_+ + h_- + h_G \quad -23b-$$

$$I = 1/2 \sum C_i Z_i^2 \quad -23c-$$

where

H_e^0 = solubility in water (litre atm./gm. mole)

I = ionic strength of the solution

h_+, h_-, h_G = contributions to h of ions and gas (l./gm.ion)

C_i = concentration of i ion species (gm. mole/l.)

Z_i = electric charge.

Henry's Law Constant for water was obtained from the "Chemical Engineers' Handbook" (18). The values of h_+, h_-, h_G were obtained from Dankwertz (12).

5. Reaction Rate Constant

Figure 13 represents the values of reaction velocity

constant as reported by Sharma (19). These values were obtained from liquid jet absorption data, and used in the work of Brian et al. (4) under pseudo first order reaction conditions. The values agree with those reported by Jensen, Jorgensen, and Faurholt (20).

6. Ionization Data of MEA in Aqueous Solution

The hydrolysis of MEA in aqueous media has been studied by Bates and Pinching (21). Figure 14 shows the calculated concentrations of hydroxyl ion and free amine in solutions of various total amine strengths.

7. Physical Absorption Liquid-Film Coefficient

An average value k_L^o (physical absorption liquid-film coefficient) was obtained from Wales (7). For the same range of flow rates, k_L^o has a mean value of 0.026 cm./sec.

IV. EXPERIMENTAL APPARATUS AND PROCEDURE

A. Description of Apparatus

A flow chart of the equipment is shown in Figure 3. The vertical test section, Figure 4, was constructed of 1/2" I.D.-3/4" O.D. clear plexiglass. The first sampling tap is located 113 pipe diameters from the entrance tee to allow a stabilized, fully developed flow pattern.

Two polyethylene tanks (each 200 gals.) were used as reservoirs for MEA solutions. A 1/4 h.p. reciprocating pump was used to deliver the solution to the test section. The liquid circuit was constructed with 1/2" tygon tubing, a bypass valve, and a liquid rotameter calibrated for water throughput.

The sour gas - a mixture of CO₂ in air - was made by passing air from the laboratory pressure line at 95 p.s.i.g. through a filter to a high accuracy Brooks rotameter (calibrated to a 1% accuracy) and mixing it with CO₂ from a cylinder. The solute gas was heated following expansion and metered through a twin float Brooks rotameter which was calibrated with a wet test meter. Flow rates of the individual streams were controlled by needle valves located at the exit end of the rotameters. To reduce fluctuations, flow chambers were connected into the circuit. Pressure, temperature, and humidity measurements were made at points indicated by the diagram.

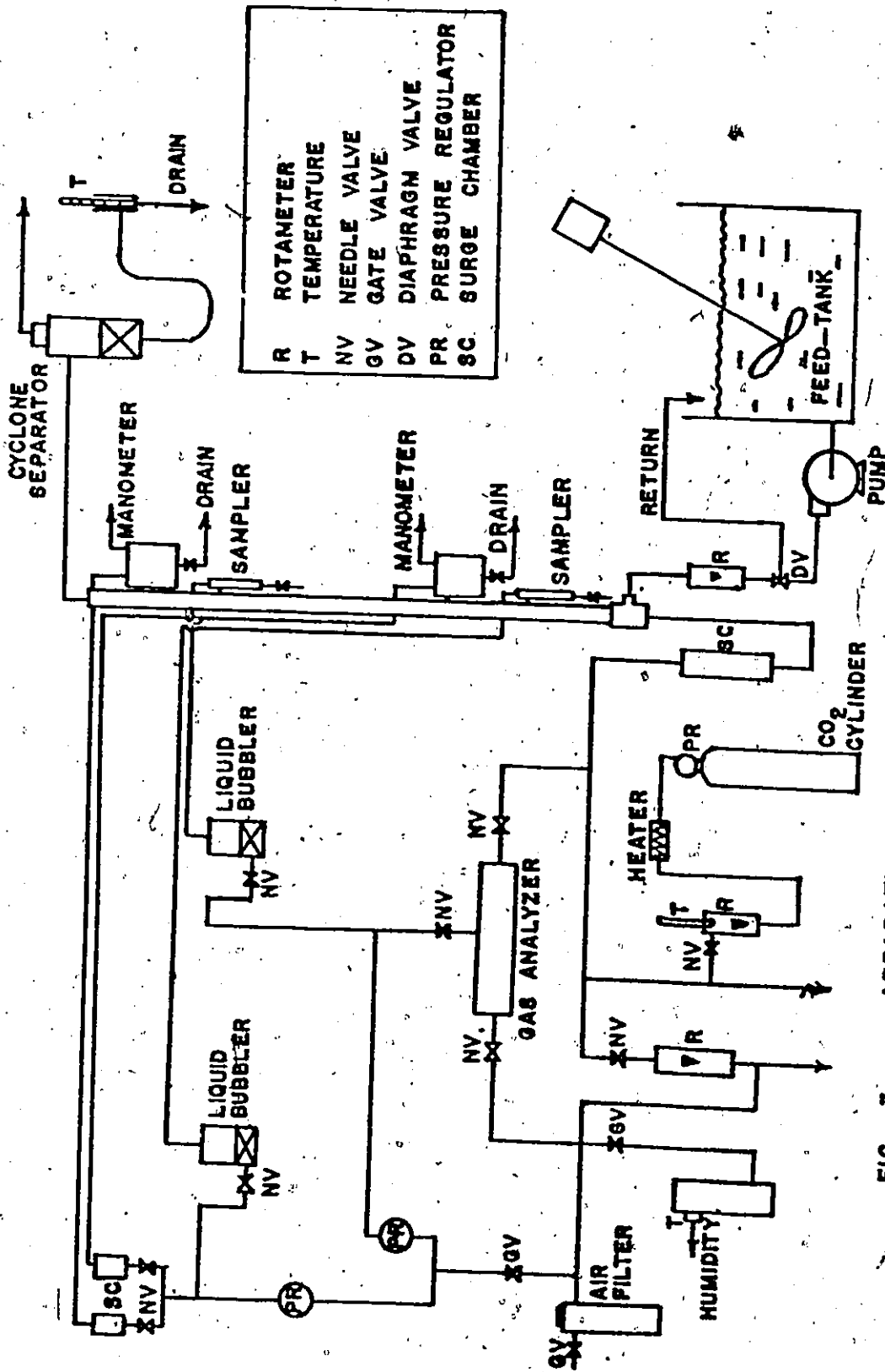


FIG. 3 APPARATUS

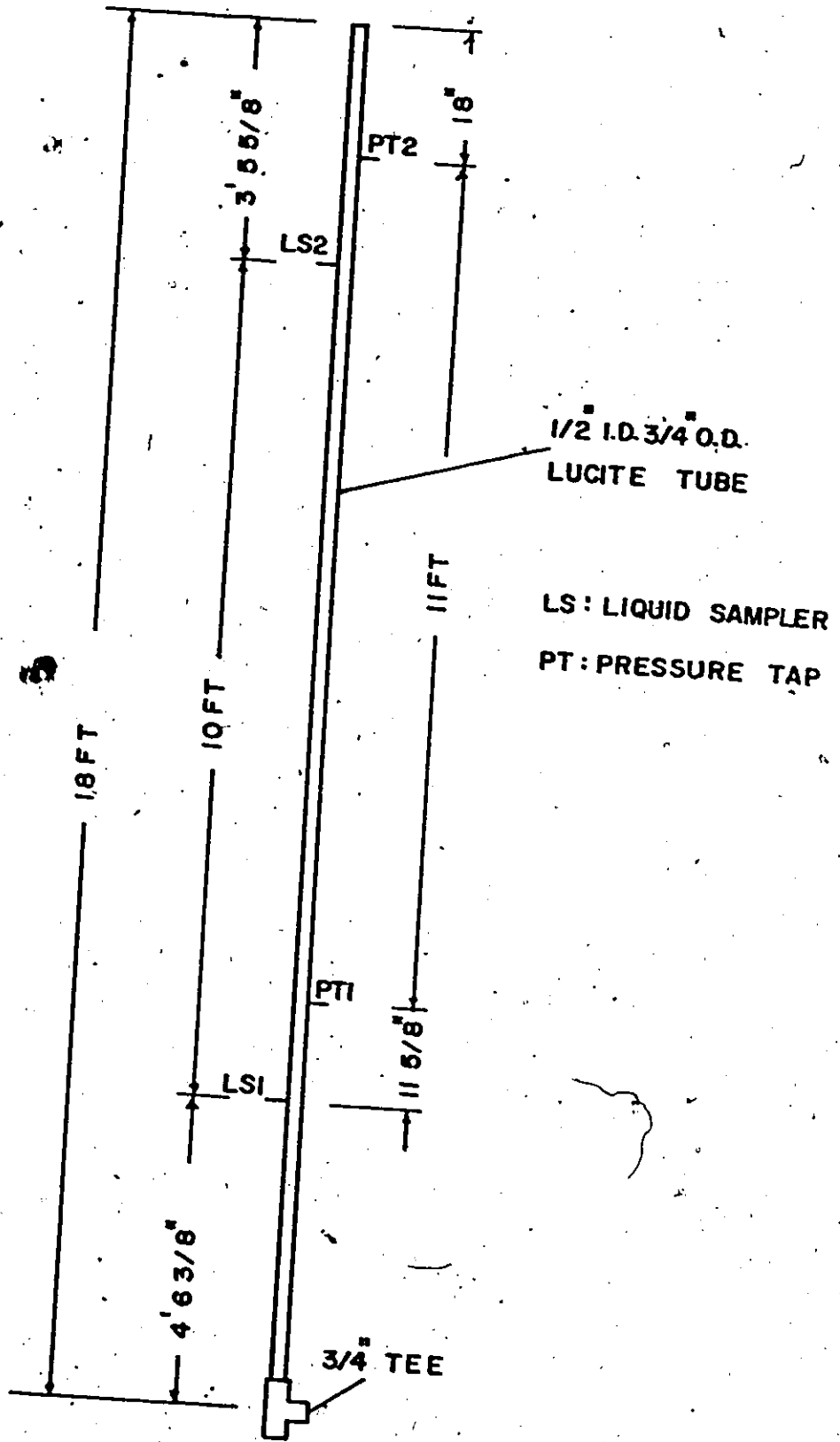


FIG. 4 TEST SECTION (NOT TO SCALE)

At the exit end of the loop a cyclone separator separated the two-phase mixture; the gas phase exiting through a 4" I.D. plastic tube to a fume hood, and the liquid phase following a return line through a liquid trap to a drain. A thermometer was installed at the trap so that liquid temperatures could be measured.

B. Pressure Measurements

Four U-type manometers provided the necessary data on pressure requirements. Two manometers loaded with mercury, recorded the pressure values for the individual gas streams and two manometers loaded with "Meriam Red Oil" (S.G. - 2.95) recorded pressure values in the column. Surge chambers and capillary tubes connected to the test column manometer lines helped to dampen pressure fluctuations. Air purge was used to balance column pressures with separator pressures. Details are shown in Figure 5.

C. Sampling Technique and Analysis

In order to evaluate the volumetric mass transfer coefficient, the amount of reacted gas between points in the column must be known. The degree of accuracy in calculating this coefficient depends on the sampling technique. The technique used, which is relatively new to mass transfer studies, was suggested by A.K. Jagota to Kahol (6) and used by the latter in the absorption studies of CO_2 in aqueous

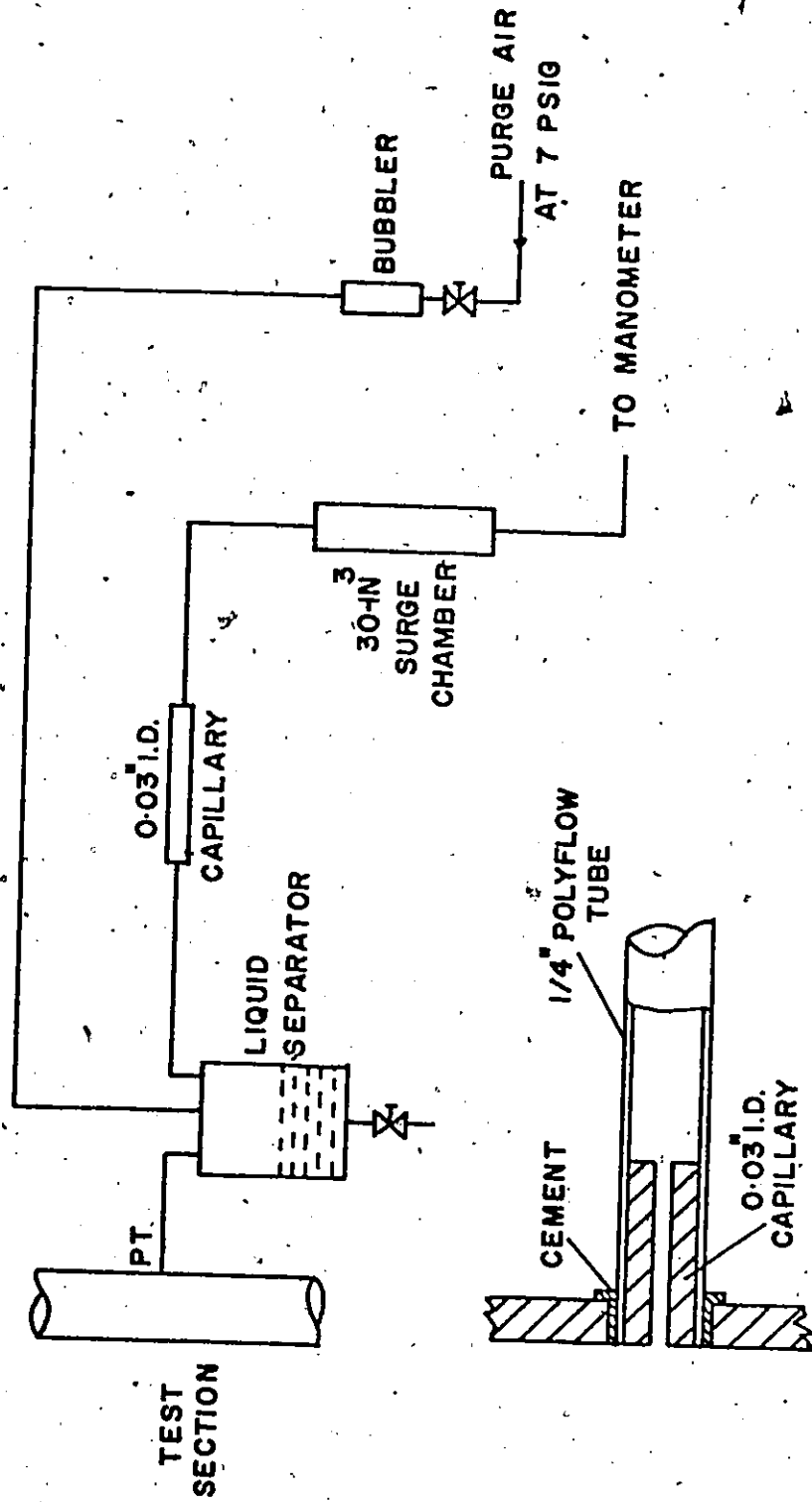


FIG. 5 PRESSURE MEASURING SYSTEM (NOT TO SCALE)

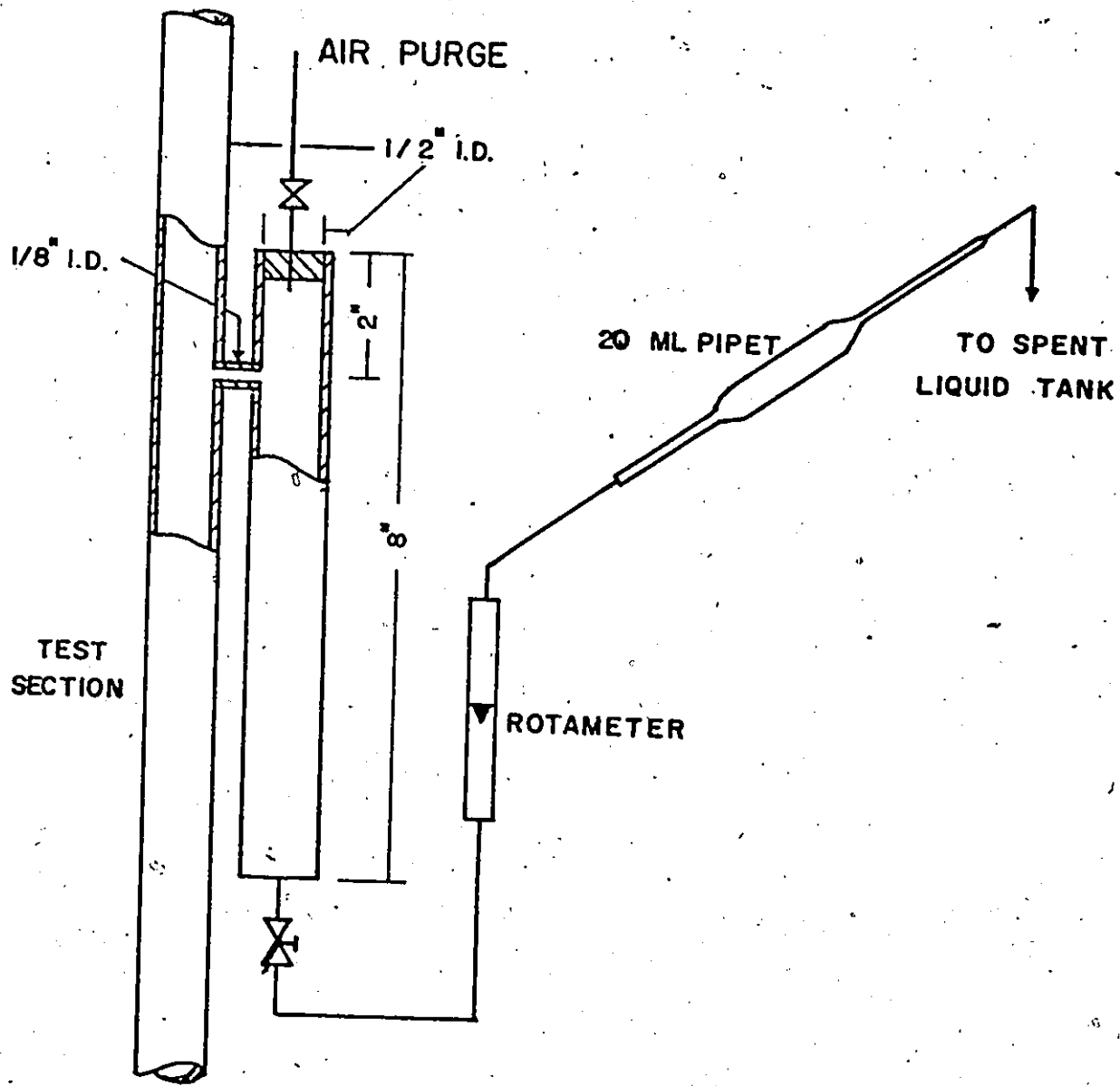


FIG. 6 GRAVITY SEPARATOR TYPE LIQUID SAMPLER

solutions of sodium hydroxide. Figure 6 illustrates the proposed gravity separator type sampler and its application to a vertical system. For the particular flow regime it offers both accuracy and reproducibility of results. In operation, the purge air was turned on to minimize the amount of gas entering the sampler, and when the liquid filled the sampler up to the level of the connecting tube, the rotameter valve was opened and the liquid was collected in a 20 c.c. pipet at a rate of 15 c.c./min. Liquid flow rates ranging 10-20 c.c./min. made negligible effect on the value of $K_G \cdot a$. To insure accuracy of results, sampler collection lag time was minimized by a continuous flow through the rotameters. A reproducibility of 10% or better in determining $K_G \cdot a$ was achieved.

The liquid samples obtained from the test section were mixed with 4 mls of saturated $BaCl_2$ solution and allowed to stand for a minimum of 2 hours. After the precipitation of $BaCO_3$ the samples were filtered and titrated with a standard 0.1 N HCl solution using bromphenol blue as the indicator. The endpoint could be determined within 0.05 c.c. of titrant.

Figure 18 illustrates the titration curve for an aqueous solution of MEA titrated with standard HCl. The purpose of the curve was only to choose the proper indicator for the system.

D. Experimental Procedure

Each experimental run involved the taking of 90 samples

from the test column. The outlined procedure was followed.

1. Both reservoir tanks were washed and loaded with an MEA solution of similar strength. Tap water was used to fill the tanks. Water samples were taken and analyzed for hardness and alkalinity.

2. The temperature and concentration of the solution was recorded. The desired value for the gas mixture was set, the purge air valves were opened, and the solution was admitted to the test section.

3. For each set value of sour gas and solution flow rate, 6 samples were taken from the column at 5 minute intervals with the liquid sampler valves set at 15 c.c./min.

4. Pressure, temperature and humidity measurements were made. The required time for the flow to become steady, measured between 1 to 2 minutes.

5. An 8 to 10 minute interval was allowed for steady state after each change in set value and sampling procedures were repeated.

V. EXPERIMENTAL RESULTS AND DISCUSSION

All experimental results are tabulated in Appendices I and II. For simplicity, it becomes convenient to breakdown the observed values and discuss them in the following parts: pressure drop, overall mass transfer coefficient, interfacial areas, liquid and gas film coefficients, and accuracy of results.

All physical properties used for calculations were based upon conditions at the midpoint of the test section.

A. Pressure Drop

Pressure drop measurements were made for air and water. The range of measurements is indicated below:

$$J_F^* - 0.92 \text{ to } 2.10$$

$$J_G^* \triangleright 0.42 \text{ to } 1.22$$

The predicted pressure gradients from Powley's correlation (22) are plotted against measured values in Figure 7. The band indicated by ± 6 (one standard deviation) indicates a measure of precision. The regime constant for the system was found to be 0.76 which agrees quite well with Powley's (22) value of 0.77 calculated for horizontal systems.

Figure 8 identifies the relationships between the Lockhart-Martenelli ϕ_{Ltt} and Wallis' (13) R_{LS} as a function of the formers' X_{tt} . Experimental data substantiates the following equations:

PRESSURE DROP CORRELATION
AIR AND WATER

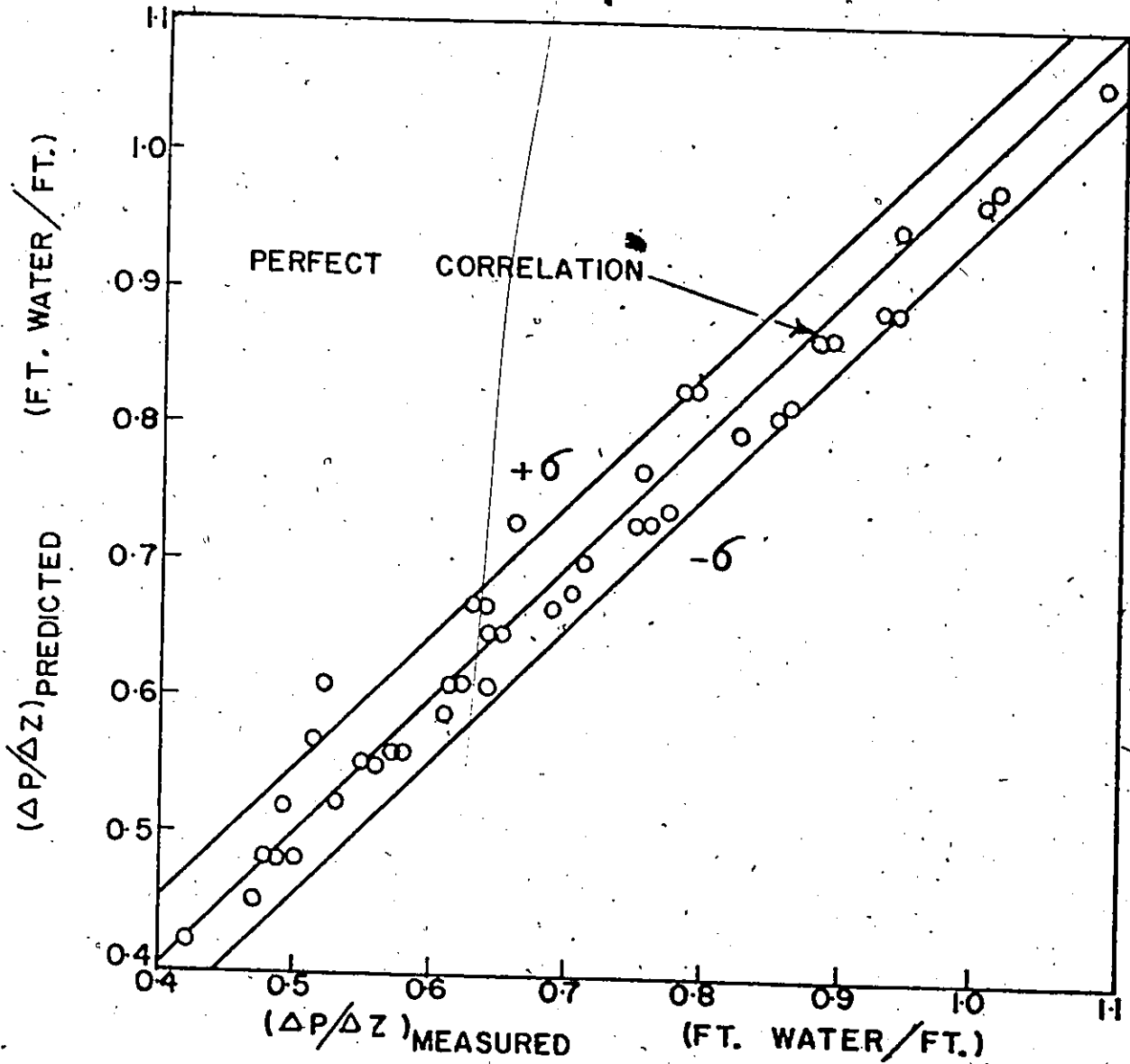


FIG. 7 COMPARISON OF POWLEY'S MODEL WITH
MEASURED VALUES $A = 0.76$
CORRELATION COEFFICIENT = 0.98

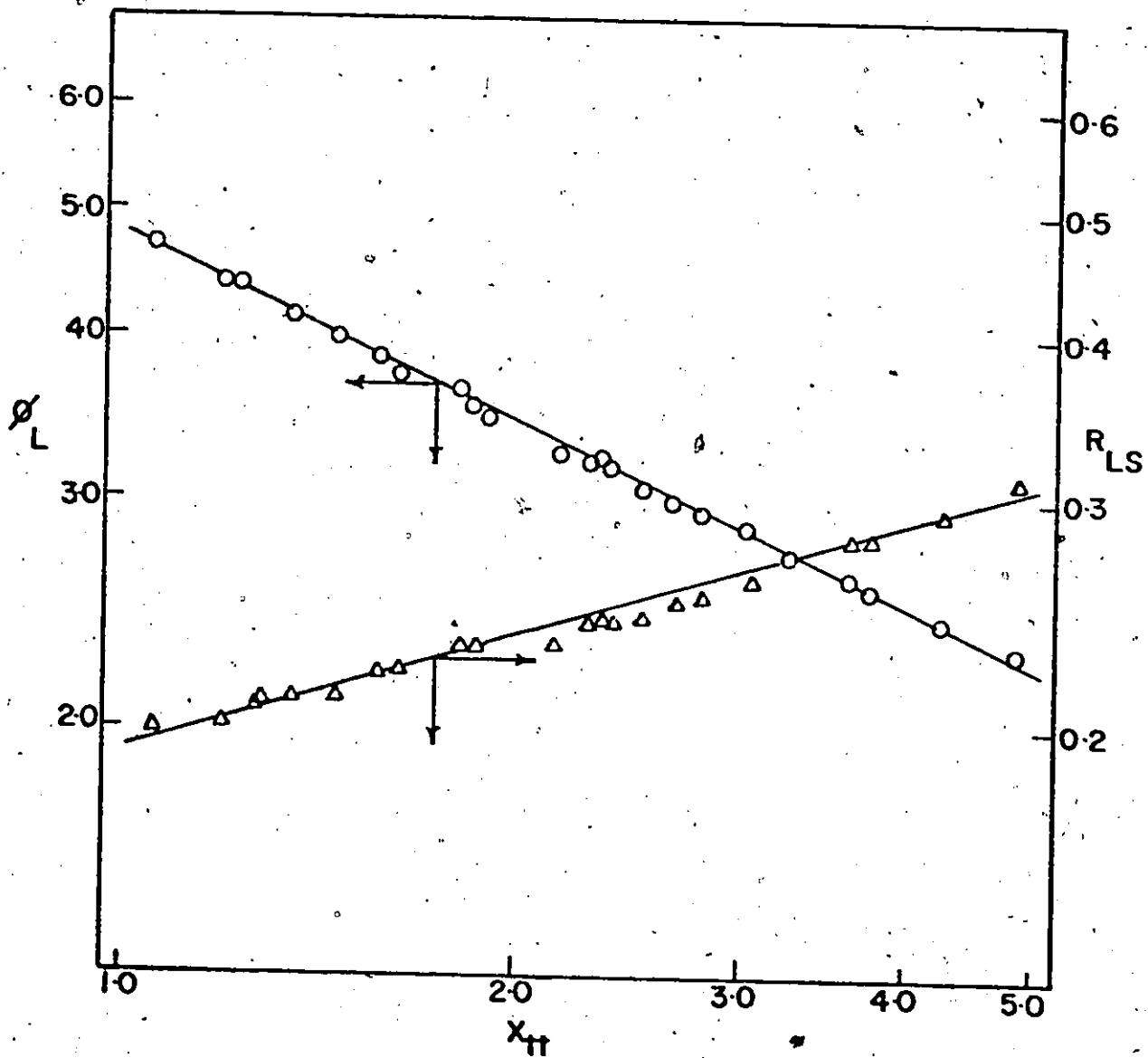


FIG. 8 ϕ_L AND R_{LS} AS A FUNCTION OF
THE LOCKHART - MARTINELLI X_{tt}

$$R_{LS} = 0.192X_{tt}^{0.281}$$

-24-

or

$$R_{LS} = \frac{0.488}{\rho_{Ltt}^{0.594}}$$

-25-

Turner (23) found equation 26 to be valid when shear stresses dominate the flow (ie. $J_G^* \gg 2$)

$$R_L = \frac{1}{\rho_L}$$

-26-

where

R_L = liquid volume fraction

To observe the variation of liquid fraction R_{LS} and R_L are recorded in Appendix I. Of further interest was R_{LA} (liquid fraction in the annular flow regime). It can be seen that in the slug flow regime R_L overestimates liquid fraction by approximately 35%. The values of R_{LS} approach that of R_{LA} with movement towards the transition-annular boundary. The low values recorded for quality is a further indication of the slug-transition regime where both gravitational and inertial forces are significant.

B. Overall Mass Transfer Coefficient

Figures 9 and 10 represent the mass transfer results obtained for the Air-CO₂-MEA system. Appendix I contains the mass transfer data with criteria for pseudo first order reaction. The experimental range for the observed values is given below:

$$j_F^* = 0.893 \text{ to } 1.746$$

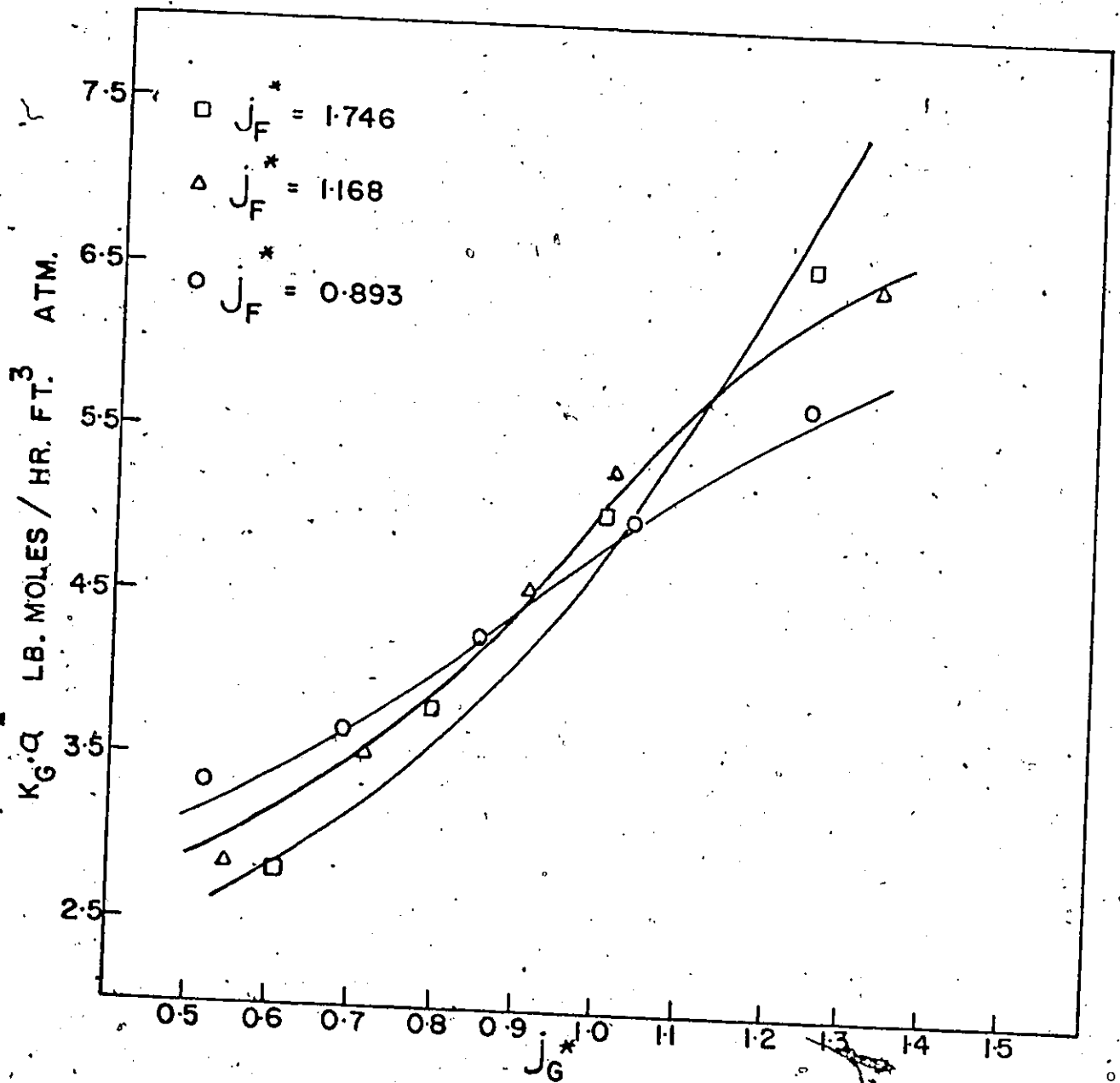


FIG. 9 EFFECT OF DIMENSIONLESS GAS AND LIQUID VELOCITIES ON OVERALL MASS TRANSFER COEFFICIENT $b_0 = 0.171$

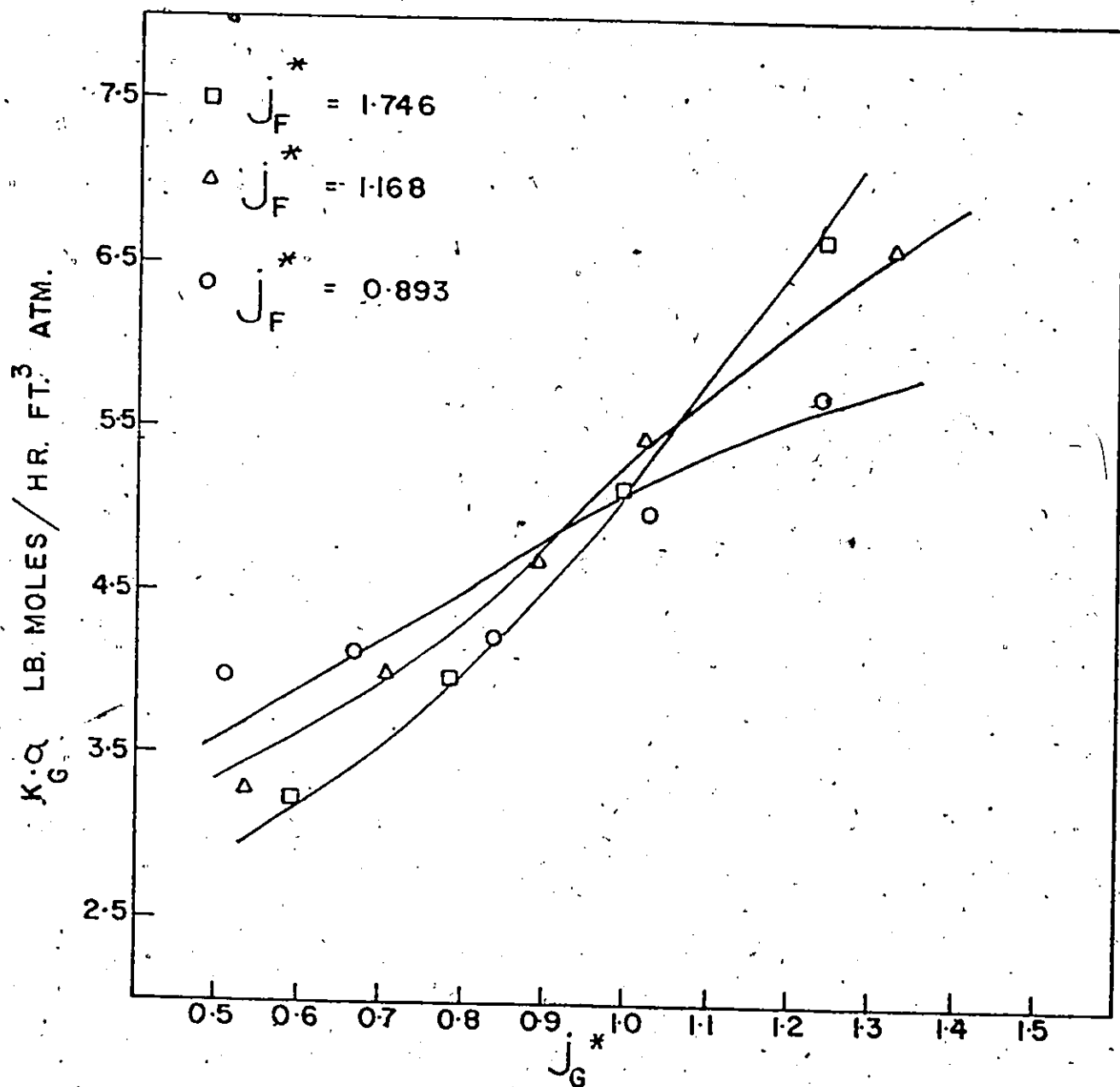


FIG. 10 EFFECT OF DIMENSIONLESS GAS AND LIQUID VELOCITIES ON OVERALL MASS TRANSFER COEFFICIENT FOR $b_0 = 0.257$

$$j_G^* - 0.510 \text{ to } 1.337$$

$$b_0 - 0.171 \text{ and } 0.257 \text{ gm. moles/litre}$$

The overall mass transfer coefficient was calculated from the following equation:

$$K_G \cdot a = \frac{Q_L(b_1 - b_2)}{32.04 P_{1m} \cdot Y_{1m} \cdot V} \quad -27-$$

where

Q_L = liquid flow rate ft.³/hr.

b_1 = MEA concentration at lower sample point gm. moles/l.

b_2 = MEA concentration at upper sample point gm. moles/l.

P_{1m} = log mean pressure in test section atm.

Y_{1m} = log mean mole fraction of CO₂ in the gas phase

V = volume of test section ft.³

In order to obtain unbiased inferences of the effects of the independent variables on $K_G \cdot a$ a regression model was fitted to the data. The model being fitted was of the form of the Taylor's series expansion of $1/K_G \cdot a$ as a function of j_F^* , j_G^* and PR.

where

$$PR = H / (Dk b_e)^{1/2} \quad -28-$$

and

$$b_e = (b_1 + b_2) / 2.0 \quad -29-$$

A standard I.B.M. program for multiple linear regression, "REGRE", was used to fit the model to experimental data. The result is of the form shown in equation 30.

$$\frac{1}{K_G \cdot a} = a_0 + a_1 PR - J_F^* (a_2 J_G^* - a_3) - J_G^* (a_4 PR - a_5 J_G^*) \quad -30-$$

The values of the coefficients and computed "t" values are indicated below in Table 1.

TABLE 1: REGRESSION COEFFICIENTS

<u>COEFFICIENT</u>	<u>VALUE OF COEFFICIENT</u>	<u>COMPUTED "t" VALUE</u>
a ₀	0.01656	----
a ₁	0.01189	5.73
a ₂	-0.16777	-6.87
a ₃	0.17041	7.47
a ₄	-0.00972	-4.57
a ₅	0.12909	-4.23

A multiple regression correlation coefficient of 0.984 was obtained. Table 2 in Appendix II summarizes the analysis of variance for the regression. The recorded values indicate a 99% chance that the total variation in $1/K_G \cdot a$ is explained by the regression model; thus, indicating a good fit.

The general trends in Figures 9 and 10 are identical. The reported values of $K_G \cdot a$ range from 3.34 - 6.63 lb.moles/hr.ft.³atm. for MEA concentrations of .171 and .257 gm.moles/l. and CO₂ concentrations ranging from 4.6 to 5.3 percent by volume. Weiland (24) has reported values for $K_G \cdot a$ ranging from 7. - 13 lb.moles/hr.ft.³atm. for ethylenediamine concen-

trations ranging from 1.6 to 4.2 gm.moles/litre and CO_2 partial pressures ranging from 0.02 to 0.03 atm.

Explanation for the observed variation in $K_G \cdot a$ can be made by considering the regime chart in Figure 1. When j_G^* is approximately less than 0.9 the flow is chaotic; that is, there is a rising and falling of the liquid-gas mixture in the column. The flow pattern is primarily influenced by gravity. An increase in gas rate in this region will increase the number of bubbles formed (i.e. increase in turbulence). The observed result is an increase in $K_G \cdot a$ through increased interfacial area. An increase in liquid rate, however, serves only to accelerate the whole system. When this occurs, gas-liquid contact time decreases and a decrease in $K_G \cdot a$ is observed.

When j_G^* becomes approximately greater than 1.1, the flow becomes stable. In this region, where inertial forces predominate, $K_G \cdot a$ increases with both j_G^* and j_P^* . In the tube the gas stream pushes the bulk of the liquid to the wall and causes entrainment of liquid droplets. An increase in liquid rate, increases the liquid layer at the wall thereby, decreasing available cross-sectional area for gas flow. As a result, there is an increase in gas velocity which in turn increases the level of entrainment. The overall effect is an increase in $K_G \cdot a$.

An increase in MEA concentration serves to decrease the liquid film thickness through increased availability of MEA

for reaction. The net effect is an increase in $K_G \cdot a$.

C. Interfacial Areas

Figure 11 illustrates the effects of fluid rates on effective interfacial area. For the region investigated, changes in liquid rates caused no effect on interfacial areas. From Figure 1, one would suspect a decrease in interfacial area with increasing liquid rate, since the move would be deeper into the slug flow regime. From this train of thought it can only be concluded that the slug-froth transition line has a much lower slope than indicated in Figure 1.

It is evident that effective interfacial area increases enormously as j_G^* becomes much greater than one. Wallis (13) indicates that entrainment values ranging from 20% to 80% are characteristic of this regime. Kahol (6) has recorded values for the same flow regime which show definite increases in "a" as a function of both v_G and v_L . Weiland (24) has measured "a" in a countercurrent absorber, packed with 1/4" Raschig rings. The values reported were approximately 60 ft.^{-1} for liquid velocity of 0.02 ft./sec. and gas velocity 1.5 ft./sec.

D. Individual Film Coefficients

At this stage it becomes significant to point out that k_L shows negligible increase as movement is made from the slug flow regime to the transition zone. However, increases of approximately 25% are observed as initial MEA concentration is increased from 0.172 to $0.257 \text{ gm. moles/litre.}$ The very large

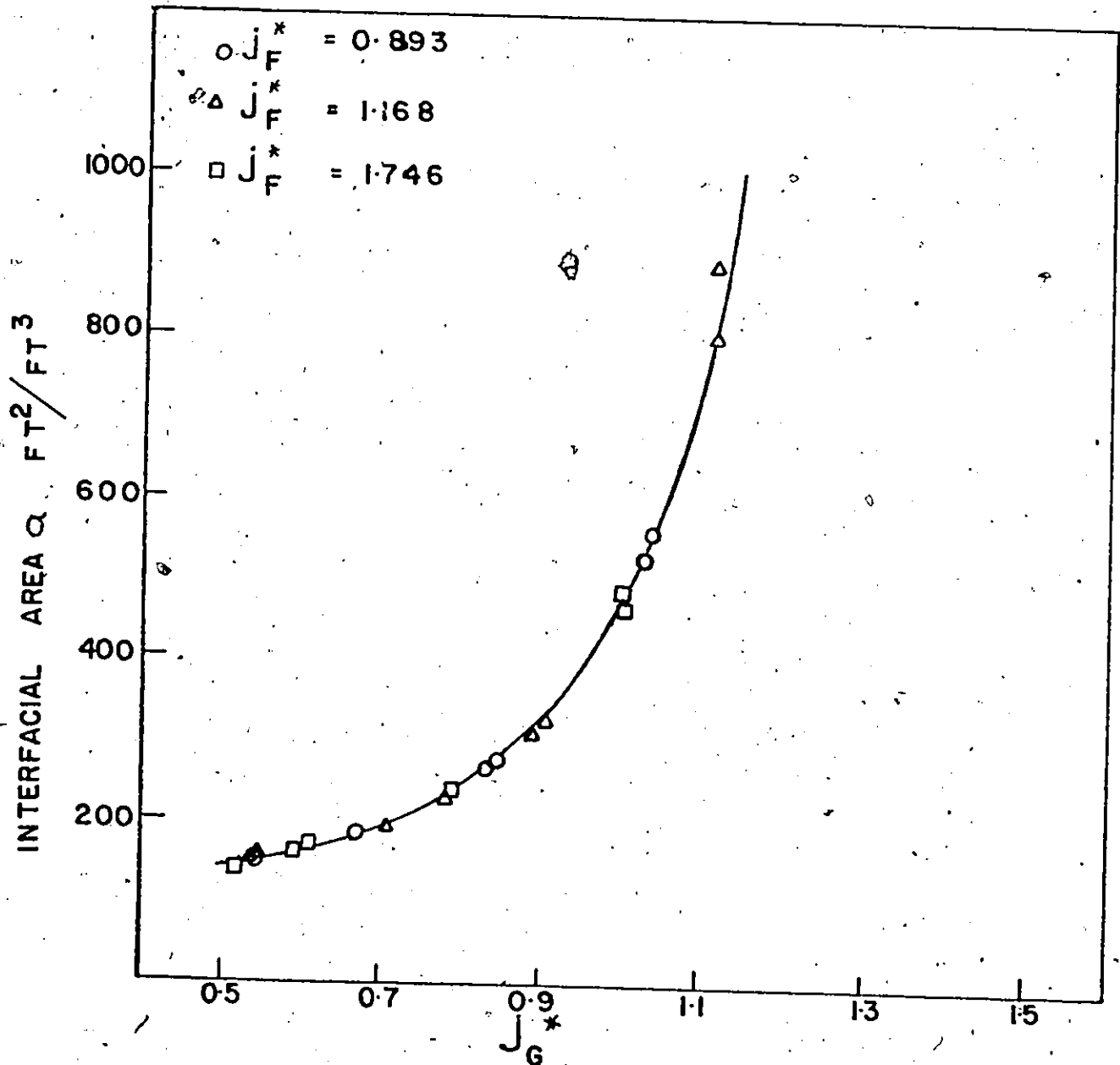


FIG. II EFFECT OF DIMENSIONLESS GAS AND LIQUID VELOCITIES ON INTERFACIAL AREA

decrease in liquid film resistance after J_G^* becomes greater than 1.1 can only be accounted for by large increases in effective interfacial area. Mass transfer at this point becomes entirely gas phase controlled.

Figure 12 indicates the relationship between the gas phase volumetric coefficient as a function of J_G^* and J_F^* . For $J_G^* < 1$ an increase in J_F^* , at constant J_G^* , causes a reduction in contact time and the value of $K_G \cdot a$ decreases. For $J_G^* > 1.1$ the reverse case holds true; that is, as J_F^* increases $K_G \cdot a$ increases. This effect can be explained by the fact that at constant J_G^* the lower values for J_F^* will reach the transition zone at a faster rate than larger values. The transition zone introduces the annular regime. This regime is characterized by entrainment of liquid droplets travelling essentially at gas velocity. The net effect is large gas film boundary layers which dictate mass transfer by diffusion only.

E. Accuracy of Results

An approximate estimate of error in the calculated values of overall mass transfer coefficient resulting from uncertainties in the independent variables of equation 27 is presented here. Table 3 represents the uncertainty limits of the experimental measurements.

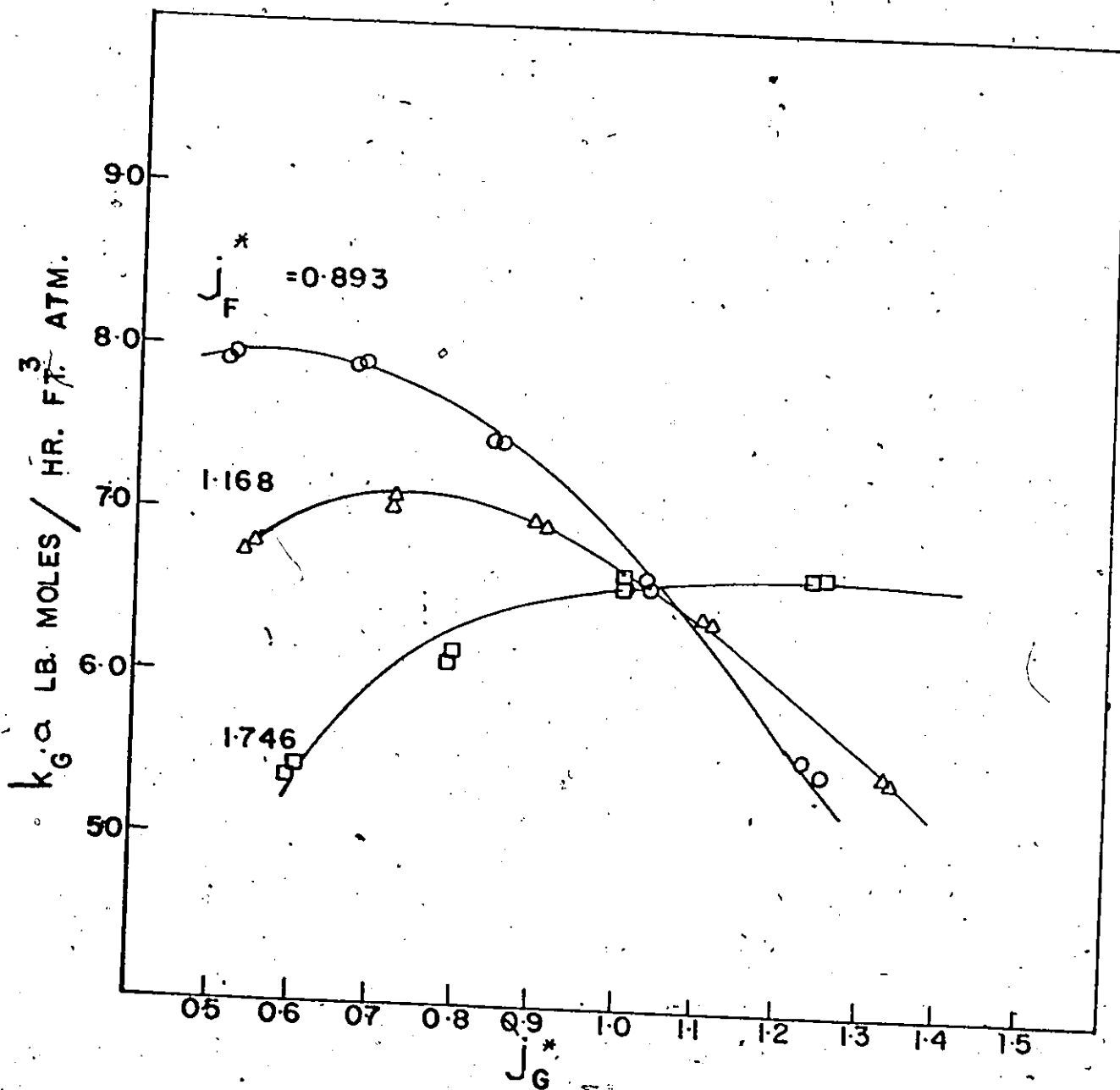


FIG. 12 EFFECT OF DIMENSIONLESS GAS AND LIQUID VELOCITIES ON THE GAS FILM COEFFICIENT

TABLE 3: UNCERTAINTY LIMITS IN VARIABLES

$$Q_L \pm 2\%$$

$$(b_1 - b_2) \pm 5\%$$

$$P_{1m} \pm 1\% \text{ (estimated)}$$

$$Y_{1m} \pm 6\%$$

The uncertainty in the overall mass transfer coefficient, calculated by the method of Holman (25), is $\pm 8.1\%$. The experimental runs repeated at random were found to be reproducible to within $\pm 10\%$. The discrepancy evident here is only due to variation in rotameter and manometer readings caused by instabilities in the two-phase flowing system.

VI. CONCLUSIONS

The chemical absorption of CO_2 from air into MEA solutions has been studied. Measurements of the overall mass transfer coefficient $K_G \cdot a$ has been made in the slug and transition flow regimes. The relative importance of the effects of flow rates and MEA concentrations have been determined and a model for the chemical absorption process has been proposed.

The gravity type liquid sampler, a relatively new sampling technique in mass transfer studies, has been evaluated and found effective for the system investigated.

By assuming a pseudo first order reaction model for the absorption of CO_2 , interfacial areas and gas film coefficients have been predicted for the experimental range of gas and liquid rates. The results obtained in this study agree in order of magnitude with those of Weiland (24), which suggests that large initial concentrations of absorbent are not necessary to obtain large transfer rates. The trends of the measured values indicate that both gravitational and inertial forces are significant in mass transfer in the slug-transition regimes.

The pressure drop studies made in this study are in good agreement with Powley's correlation which makes use of a regime constant. A new method for estimation of liquid volume fraction based on Lockhart-Martenelli parameters has been proposed for vertical two-phase flow.

NOMENCLATURE

MEA	Monoethanolamine ($\text{HO}-\text{CH}_2-\text{CH}_2-\text{NH}_2$)
b	Concentration of MEA gm.moles/litre
PR	Defined by equation 28
d	Diameter of tube ft.
D	Diffusion coefficient $\text{cm.}^2/\text{sec.}$
x	Distance from interface ft.
X	Average quality
X	Association parameter equal to 2.6 for water
X_{tt}	Lockhart-Martenelli parameter for turbulent-turbulent flow defined by equation 15
k	Reaction rate constant l./gm.mole sec.
k'	Pseudo rate constant sec.^{-1}
l	Length between pressure taps ft.
Z	Stoichiometric factor
k_L^0	Liquid film coefficient for physical absorption $\text{cm.}/\text{sec.}$
k_L	Liquid film coefficient for chemical absorption $\text{ft.}/\text{hr.}$
k_G	Gas film coefficient for mass transfer $\text{lb.moles}/\text{hr. ft.}^2 \text{ atm.}$
a	Effective interfacial area for mass transfer $\text{ft.}^2/\text{ft.}^3$
$K_G \cdot a$	Overall volumetric mass transfer coefficient $\text{lb.moles}/\text{hr. ft.}^3 \text{ atm.}$
N	Absorption rate per unit interfacial area $\text{lb.moles}/\text{ft.}^2$
m	Slope of equilibrium curve for CO_2 -water system $\text{l.atm.}/\text{gm.mole}$

M	Molecular weight of solvent
He ⁰	Henry's Law constant for CO ₂ -water system 1.atm./gm.mole
He	Henry's Law constant for CO ₂ -MEA system 1.atm./gm.mole
h ₊ , h ₋ , h _G	Contributions to h of ions and gas l./gm. ion
h	Defined by equation 23b
C _i	Concentration of i ion species gm.mole/l.
Z _i	Electric charge of i species
I	Ionic strength of solution, defined by equation 23c
T	Temperature in °K.
v	Molecular volume of solute at the normal boiling point cm. ³ /gm.mole
V	Volume of test section ft. ³
μ	Viscosity of solution cp.
dp/dz	Pressure gradient lb _f /ft. ³
(dp/dz) _f	Frictional pressure gradient lb _f /ft. ³
A	Flow regime constant
R _L	Liquid volume fraction defined by equation 26
R _{LS}	Liquid volume fraction for slug flow regime defined by equation 18a
R _{LA}	Liquid volume fraction for annular flow regime defined by Wallis (13)
g	Acceleration due to gravity ft./sec. ²
g _c	Gravitational constant 32.2 lb _m ft./lb _f sec. ²
G	Total mass flux lb_m/hr.ft.²
P	Pressure atm.
v	Superficial velocity ft./hr.

- J_F^* Dimensionless liquid velocity as defined by equation 18b
- J_G^* Dimensionless gas velocity as defined by equation 18a
- Q_L Volumetric liquid flow rate, ft.³/hr.
- Y Mole fraction of CO₂ in gas phase

Greek Symbols

- δ_L Critical distance from interface which defines liquid bulk, ft.
- ρ Density lb_m/ft.³
- σ Standard deviation
- ϕ_{Ltt} Empirical function of X_{tt} defined by equation 17

Subscripts

- 0 Initial value
- 1 At lower sampling point
- 2 At upper sampling point
- o Average value defined by equation 29
- lm. Log mean value
- e Equilibrium value
- T Total
- M Momentum
- E Elevation
- LP, L, F Liquid phase
- GP, G Gas phase
- TPF Two-phase friction
- G_{in} Gas phase at lower pressure tap

in Lower pressure tap
out Upper pressure tap
CA CO₂ in MEA
CW CO₂ in water
AA MEA in MEA solution
AW MEA in water

REFERENCES

1. Wallis G., Eleventh Advanced Seminar, Two-Phase Gas Liquid Flows, A.I.Ch.E., New York, pp 1-33 (1967).
2. Heuss, J.M., C.J. King and C.R. Wilke, A.I.Ch.E. Journal, 11, 866, (1965).
3. Emmert, R.E. and R.L. Pigford, A.I.Ch.E. Journal, 8, 171, (1962).
4. Brian, P.L.T., J.E. Vivian and D.C. Matiotos, A.I.Ch.E. Journal, 13, 28, (1967).
5. Van Heuver, J.W. and W.J. Beek, Chem. Eng.Sci., 18, 377 (1963).
6. Kahol, A.P., Master Thesis, University of Windsor, Windsor Ont., (1969).
7. Wales, C.E., A.I.Ch.E. Journal, 12, 1166 (1966).
8. Bradley, K.J. and H. Andre, Canadian Journal of Chemical Engineering, 50, 528 (1972).
9. Astarita, G., Mass Transfer with Chemical Reaction, Elsevier Publishing Co., Amsterdam (1967).
10. Dankwertz, P.V. and K.M. McNeil, Trans. Inst. Chem. Engrs., 45, T32 (1967).
11. Pinsent, B.R., L. Pearson and F.J.W. Roughton, Trans. Far. Soc., 52, 1512 (1956).
12. Dankwertz, P.V., Gas-Liquid Reactions, McGraw Hill Publishing Co., N.Y. (1970).
13. Wallis, G.B., One Dimensional Two-Phase Flow, McGraw Hill Publishing Co., N.Y. (1969), p.345.
14. CRC Handbook of Chemistry and Physics, 49th ed., Published by The Chemical Rubber Co., Cleveland, Ohio. (1968).
15. Thomas, W.J. and I.A. Furzer, Chem. Eng. Sci., 17, 115 (1962).
16. Wilke, C.R. and P. Chang, A.I.Ch.E. Journal, 1, 264 (1955).

17. Dankwertz, P.V. and M.M. Sharma, The Chemical Engineer, CE 244, October (1966).
18. Perry's Chemical Engineers' Handbook, 4th ed., McGraw Hill Publishing Co., N.Y. (1963).
19. Sharma, M.M., Ph.D. thesis, University of Cambridge, England (1964).
20. Jensen, M.B., E. Jorgensen and C. Faurholt, Acta. Chem. Scand., 8, 1137 (1954).
21. Bates, R.G. and G.D. Pinching, Journal, Research Natl. Bur. Standards, 46, 349 (1951).
22. Powley, M.B., Two-Phase Flow, presented at the 15th Canadian Chemical Engineering Conference, Quebec City, Quebec, October (1965).
23. Turner, J.M., Ph.D. thesis, Dartmouth College, Hanover, N.H., (1966).
24. Weiland, R.H., Ph.D. thesis, University of Toronto, Toronto, Canada, (1968).
25. Holman, J.P., Experimental Methods for Engineers, McGraw Hill Publishing Co., N.Y., (1966), p.37.

APPENDIX I
COMPUTER PROGRAM LISTING AND OUTPUT


```

57 C MEA CONC IN LIQUID
58 B1=SOL*V1/SAM
    B2=SOL*V2/SAM
C CALC OF DRIVING FORCE
C DC1=LB. MOLES CO2 ABSORBED AT LOWER TEST POINT (MOLES/HR.)
C CONVERSION CONSTANT 32.04 INCLUDES STOICHIOMETRIC FACTOR
C CM1=FLOWRATE OF CO2 AT LOWER TEST POINT (MOLES/HR.)
C YC1=MOLE FRACTION OF CO2 IN GAS PHASE AT LOWER TEST POINT
C DC2=LB. MOLES OF CO2 ABSORBED BETWEEN TEST POINTS (MOLES/HR.)
C CM2=FLOWRATE OF CO2 AT UPPER TEST POINT (MOLES/HR.)
C YC2=MOLE FRACTION OF CO2 IN GAS PHASE AT UPPER TEST POINT
59 DC1=OLC*(B1-B01)/32.04
60 CM1=CM0-DC1
61 YC1=CM1/(AM*WM+CM1)
62 DC2=OLC*(B2-B02)/32.04
63 CM2=CM1-DC2
64 YC2=CM2/(AM*WM+CM2)
65 IF (YC1-YC2) 43,43.46
66 43 PRINT 44
67 GO TO 5
68 45 CONTINUE
69 YLM=(YC1-YC2)/(ALOG(YC1/YC2))
C CALC OF VOLUMETRIC MASS TRANSFER COEFF. (LB. MOLES/HR. CU. FT. ATM.)
70 AKGA=OLC*(B1-B2)*14.7/(32.04*PB*YLM*V)
71 RECIP=1.0/AKGA
C.....
72 TC=(ST-32.0)/1.8
73 TK=273.2+TC
C CALCULATION OF HENRYS LAW CONSTANT
C HED=HENRYS LAW CONSTANT FOR CO2-WATER
C A1=IONIC STRENGTH OF SOLUTION
C H=CONTRIBUTIONS TO H OF IONS AND GAS (L./CM.ION)
74 HED=0.65*TC+12.60
75 HG=-0.0009*TC+0.0035
76 A11=0.5*(BP+BP)
77 H1=0.028+0.066*HG
78 A12=0.5*((0.001*PPH/40.0)*4.0+(0.001*PPH/60.0)*4.0)
79 H2=0.053+0.021*HG
80 A13=0.5*((0.001*ALK/23.0)+0.001*ALK/61.0)
81 H3=0.091+0.021*HG
82 S1H=A11*H1+A12*H2+A13*H3
83 HEC=HEU*(10.0*S1H)
C CALCULATION OF DIFFUSION COEFF. (SQ. CM./SEC.)
84 DCW=(7.4E-8)*SQRT(2.6+18.0)*TK/(MU*((34.0)*0.6))
85 DCA=DAA*DCW/DAA
C BLN=AVERAGE CONC. OF MEA IN TEST SECTION
C DETERMINATION OF CRITERIA FOR PSEUDO FIRST ORDER REACTION
86 BLN=(B1+B2)/2.0
87 EF=SQRT(DCA*AK*BLN)
88 EFF=EF/AKLD
89 CSTAR=PPCO2/HEC
90 CRIT=0.2/(2.0*CSTAR)+1.0
C UNITS OF PH=ATM*(FT.**2)/HR./(LB.MOLE)
91 PR=(HEC/EF)*((1000.0*454.0)/(3600.0*((12.5+12.0)**2)))
C CALCULATION OF REL
92 DIA=D
93 REL=(D*VL*62.4)/(MU*0.000672)
C CALCULATION OF REG
94 GDEN=0.07528*PB*528.0/(14.7*(460.0+ST))
95 REG=D*VGG*GDEN/(GV15*0.000672)
C CALCULATION OF DIMENSIONLESS VELOCITIES
96 VLO=VL
97 VGO=VGG
98 DIV=SQRT(32.16*DIA*(SG*2.4-GDEN))
99 AJF=VLO*SQRT(SG*62.4)/DIV
100 AJG=VGO*SQRT(GDEN)/DIV
C CALCULATION OF PARAMETERS FOR REGRESSION PROGRAM
101 X1=AJF
102 X2=AJG
103 X3=PR
104 X4=X1**2.0
105 X5=X2**2.0
106 X6=X3**2.0
107 X7=X1*X2
108 X8=X1*X3
109 X9=X2*X3
C.....
110 PRINT 77,VGGG,PCO2,OLC,AJF,AJG,PR,B1,B2,EF,CM1,PR,AKGA
111 IF (N-J) 2,5,5
112 5 CONTINUE
113 IF (K-2) 17,16,16
114 17 CONTINUE
115 GO TO 13
116 18 CONTINUE
117 STOP
118 END

```

CALCULATION OF OVERALL MASS TRANSFER COEFFICIENT

AIR	PO2	OLC	JF*	JG*	PLM	B1	B2	EFF	CRIT	PR	KGA
INLET MEA CONCENTRATION = 0.171 GM. MOLE/LITRE											
82.3	5.3	5.21	0.89	0.52	16.5	0.153	0.134	4.92	25.33	27.3	3.34
106.6	5.3	5.21	0.89	0.68	16.6	0.151	0.132	4.89	24.20	27.5	3.71
133.3	5.1	5.21	0.89	0.85	16.8	0.150	0.128	4.84	23.35	27.7	4.26
162.6	5.0	5.21	0.89	1.04	16.9	0.151	0.126	4.83	22.36	27.8	5.00
195.4	4.9	5.21	0.89	1.25	17.0	0.151	0.123	4.81	21.53	27.9	5.72
85.3	5.2	6.81	1.17	0.54	16.8	0.154	0.142	5.00	26.14	26.9	2.86
111.1	5.1	6.81	1.17	0.71	17.0	0.153	0.138	4.96	25.12	27.1	3.50
140.0	5.0	6.81	1.17	0.90	17.2	0.152	0.134	4.92	23.55	27.3	4.55
171.0	4.9	6.81	1.17	1.11	17.4	0.152	0.132	4.89	22.86	27.4	5.29
205.8	4.7	6.81	1.17	1.34	17.5	0.151	0.127	4.85	21.79	27.7	6.48
92.3	5.0	10.18	1.75	0.60	17.6	0.156	0.147	5.06	26.23	26.5	2.82
120.5	5.0	10.18	1.75	0.79	17.8	0.156	0.144	5.04	24.86	26.7	3.82
152.0	4.8	10.18	1.75	1.01	18.1	0.155	0.141	5.00	23.98	26.9	5.01
187.1	4.6	10.18	1.75	1.25	18.4	0.155	0.137	4.96	22.98	27.0	6.56

INLET MEA CONCENTRATION = 0.257 GM. MOLE/LITRE											
81.6	5.4	5.21	0.89	0.51	16.4	0.237	0.215	6.81	43.42	21.7	3.99
106.5	5.2	5.21	0.89	0.67	16.6	0.234	0.212	6.78	42.01	21.8	4.11
132.5	5.1	5.21	0.89	0.84	16.7	0.233	0.211	6.75	41.34	21.9	4.25
162.0	5.0	5.21	0.89	1.03	16.8	0.233	0.208	6.73	39.72	21.9	4.98
194.3	4.9	5.21	0.89	1.23	16.9	0.233	0.205	6.71	38.38	22.0	5.69
84.6	5.2	6.81	1.17	0.53	16.7	0.236	0.221	6.86	44.04	21.5	3.28
110.9	5.1	6.81	1.17	0.71	17.0	0.235	0.218	6.83	42.69	21.6	4.01
138.9	5.0	6.81	1.17	0.89	17.2	0.234	0.215	6.79	40.68	21.7	4.57
170.0	4.9	6.81	1.17	1.09	17.4	0.233	0.212	6.76	39.56	21.8	5.44
204.7	4.7	6.81	1.17	1.32	17.6	0.234	0.208	6.74	38.08	21.9	6.61
91.4	5.0	10.18	1.75	0.59	17.5	0.238	0.228	6.92	43.63	21.3	3.24
120.5	4.9	10.18	1.75	0.79	17.8	0.238	0.226	6.90	41.87	21.4	3.96
151.9	4.8	10.18	1.75	1.00	18.1	0.237	0.222	6.87	39.98	21.5	5.10
186.7	4.7	10.18	1.75	1.24	18.4	0.237	0.218	6.84	38.09	21.6	6.63

PRESSURE DROP DATA - AIR AND WATER

JF*	JG*	PDM	XTT	FI	PDF	POE	PDA	PDC	RL	RLS	RLA	X
0.92	0.42	0.42	2.36	3.19	1.87	2.70	0.01	0.42	0.31	0.24	0.28	0.016
0.92	0.42	0.43	2.35	3.19	1.88	2.70	0.01	0.42	0.31	0.24	0.28	0.016
0.92	0.56	0.47	1.81	3.61	2.39	2.50	0.01	0.45	0.28	0.23	0.25	0.022
0.92	0.56	0.47	1.81	3.60	2.39	2.50	0.01	0.45	0.28	0.23	0.25	0.022
0.91	0.71	0.50	1.47	3.98	2.90	2.37	0.02	0.48	0.25	0.21	0.24	0.027
0.91	0.71	0.49	1.47	3.98	2.90	2.37	0.01	0.48	0.25	0.21	0.24	0.027
0.91	0.86	0.49	1.23	4.33	3.43	2.29	0.02	0.52	0.23	0.21	0.22	0.033
0.91	0.86	0.49	1.23	4.33	3.44	2.28	0.02	0.52	0.23	0.21	0.22	0.033
0.91	1.02	0.51	1.05	4.67	3.99	2.22	0.02	0.57	0.21	0.20	0.20	0.039
0.91	1.02	0.51	1.05	4.66	3.99	2.22	0.02	0.57	0.21	0.20	0.20	0.039
0.91	1.19	0.52	0.92	4.99	4.56	2.17	0.03	0.61	0.20	0.20	0.18	0.045
0.91	1.19	0.52	0.92	4.99	4.56	2.17	0.03	0.61	0.20	0.20	0.18	0.045
1.21	0.42	0.48	3.02	2.85	2.40	2.89	0.01	0.48	0.35	0.26	0.29	0.012
1.21	0.42	0.48	3.01	2.85	2.40	2.89	0.01	0.48	0.35	0.26	0.29	0.012
1.21	0.56	0.53	2.31	3.21	3.04	2.65	0.02	0.52	0.31	0.24	0.27	0.017
1.21	0.56	0.53	2.31	3.21	3.04	2.65	0.02	0.52	0.31	0.24	0.27	0.017
1.21	0.71	0.57	1.86	3.53	3.70	2.49	0.02	0.56	0.28	0.23	0.25	0.021
1.21	0.71	0.58	1.87	3.53	3.69	2.49	0.02	0.56	0.28	0.23	0.25	0.021
1.21	0.87	0.61	1.57	3.83	4.34	2.39	0.03	0.61	0.26	0.22	0.23	0.026
1.21	0.87	0.62	1.57	3.83	4.34	2.39	0.03	0.61	0.26	0.22	0.23	0.026
1.20	1.02	0.64	1.35	4.11	5.00	2.31	0.04	0.67	0.24	0.21	0.22	0.030
1.20	1.02	0.63	1.35	4.11	4.99	2.31	0.04	0.67	0.24	0.21	0.22	0.030
1.20	1.19	0.66	1.18	4.39	5.69	2.25	0.04	0.73	0.23	0.20	0.20	0.035
1.20	1.19	0.66	1.18	4.39	5.69	2.25	0.04	0.73	0.23	0.20	0.20	0.035
1.50	0.42	0.55	3.64	2.61	2.94	3.06	0.02	0.55	0.38	0.28	0.29	0.010
1.50	0.42	0.56	3.64	2.61	2.93	3.07	0.02	0.55	0.38	0.28	0.29	0.010
1.50	0.57	0.61	2.79	2.93	3.69	2.79	0.02	0.59	0.34	0.25	0.28	0.014
1.50	0.57	0.61	2.79	2.93	3.70	2.79	0.02	0.59	0.34	0.25	0.28	0.014
1.50	0.72	0.65	2.26	3.22	4.46	2.61	0.03	0.65	0.31	0.24	0.26	0.017
1.50	0.72	0.64	2.26	3.22	4.46	2.61	0.03	0.65	0.31	0.24	0.26	0.017
1.50	0.87	0.71	1.90	3.48	5.21	2.49	0.04	0.70	0.29	0.23	0.25	0.021
1.50	0.87	0.71	1.90	3.48	5.20	2.49	0.04	0.70	0.29	0.23	0.25	0.021
1.50	1.03	0.75	1.63	3.74	6.00	2.40	0.05	0.77	0.27	0.22	0.23	0.025
1.50	1.03	0.75	1.63	3.73	5.98	2.40	0.05	0.77	0.27	0.22	0.23	0.025
1.49	1.20	0.79	1.42	3.98	6.79	2.33	0.06	0.83	0.25	0.21	0.22	0.029
1.49	1.20	0.78	1.43	3.98	6.78	2.33	0.06	0.83	0.25	0.21	0.22	0.029
1.80	0.42	0.64	4.28	2.43	3.50	3.24	0.02	0.61	0.41	0.29	0.30	0.009
1.80	0.42	0.64	4.28	2.43	3.50	3.24	0.02	0.61	0.41	0.29	0.30	0.009
1.80	0.57	0.69	3.27	2.72	4.38	2.93	0.03	0.67	0.37	0.27	0.28	0.012
1.80	0.57	0.69	3.27	2.72	4.39	2.93	0.03	0.67	0.37	0.27	0.28	0.012
1.80	0.72	0.75	2.65	2.98	5.26	2.73	0.04	0.73	0.34	0.25	0.27	0.015
1.80	0.72	0.76	2.65	2.98	5.26	2.73	0.04	0.73	0.34	0.25	0.27	0.015
1.80	0.88	0.82	2.22	3.22	6.14	2.59	0.06	0.80	0.31	0.23	0.26	0.018
1.80	0.88	0.82	2.23	3.22	6.14	2.59	0.06	0.80	0.31	0.23	0.26	0.018
1.80	1.04	0.88	1.92	3.45	7.01	2.49	0.07	0.87	0.29	0.23	0.24	0.021
1.80	1.03	0.89	1.92	3.45	7.01	2.49	0.07	0.87	0.29	0.23	0.24	0.021
1.80	1.20	0.94	1.67	3.66	7.92	2.40	0.09	0.95	0.27	0.22	0.23	0.025
1.80	1.20	0.94	1.67	3.66	7.92	2.40	0.09	0.95	0.27	0.22	0.23	0.025
2.10	0.43	0.70	4.88	2.30	4.07	3.40	0.03	0.68	0.44	0.31	0.30	0.007
2.10	0.43	0.70	4.90	2.29	4.05	3.41	0.03	0.68	0.44	0.31	0.30	0.007
2.10	0.58	0.77	3.73	2.57	5.07	3.06	0.04	0.74	0.39	0.28	0.29	0.010
2.10	0.57	0.77	3.74	2.56	5.06	3.06	0.04	0.74	0.39	0.28	0.29	0.010
2.10	0.73	0.86	3.01	2.81	6.08	2.84	0.06	0.82	0.36	0.26	0.28	0.013
2.10	0.73	0.85	3.02	2.80	6.06	2.84	0.05	0.81	0.36	0.26	0.28	0.013
2.09	0.89	0.94	2.52	3.03	7.08	2.68	0.07	0.89	0.33	0.24	0.26	0.016
2.09	0.89	0.93	2.53	3.03	7.06	2.68	0.07	0.89	0.33	0.24	0.26	0.016
2.09	1.05	1.01	2.17	3.24	8.07	2.57	0.09	0.98	0.31	0.23	0.25	0.019
2.09	1.05	1.00	2.18	3.23	8.05	2.57	0.09	0.98	0.31	0.23	0.25	0.019
2.09	1.22	1.09	1.90	3.44	9.08	2.48	0.11	1.06	0.29	0.22	0.24	0.022
2.09	1.22	1.10	1.90	3.44	9.08	2.48	0.11	1.06	0.29	0.22	0.24	0.022

A=0.76 CORRELATION COEFF. =0.98 SUM OF RESIDUALS SQUARES =0.063

NOMANCLATURE FOR COMPUTER OUTPUT

AIR	Flowrate of gas stream S.C.F.H.
PCO2	% CO ₂ in gas stream
QLC	Corrected liquid flowrate U.S.G.M.
JF*	Dimensionless liquid velocity
JG*	Dimensionless gas velocity
PLM	Log mean pressure in test section p.s.i.a.
B1	Concentration of MEA at lower test point gm. moles/l.
B2	Concentration of MEA at upper test point gm. moles/l.
EFF	Defined by left side of equation 11
CRIT	Defined by right side of equation 11
KGA	K _G .a
PDM	Measured pressure gradient ft. water/ft.
XTT	X _{tt}
FI	O _{Ltt}
PDF	Frictional pressure gradient ft. water/ft.
PDE	Elevational pressure gradient ft. water/ft.
PDA	Accelerational pressure gradient ft. water/ft.
RL	R _L
RLS	R _{LS}
RLA	R _{LA}
X	Quality
PR	Defined by equation 28.

APPENDIX II

TABLE 2: ANALYSIS OF VARIANCE FOR THE REGRESSION

<u>SOURCE OF VARIATION</u>	<u>DEGREES OF FREEDOM</u>	<u>SUM OF SQUARES</u>	<u>MEAN SQUARES</u>	<u>F VALUE</u>
Attributable to Regression	5	0.08888	0.01778	137.185
Deviation from Regression	22	0.00285	0.00013	
Total	27	0.09173	-----	

APPENDIX III
SYSTEM PARAMETERS

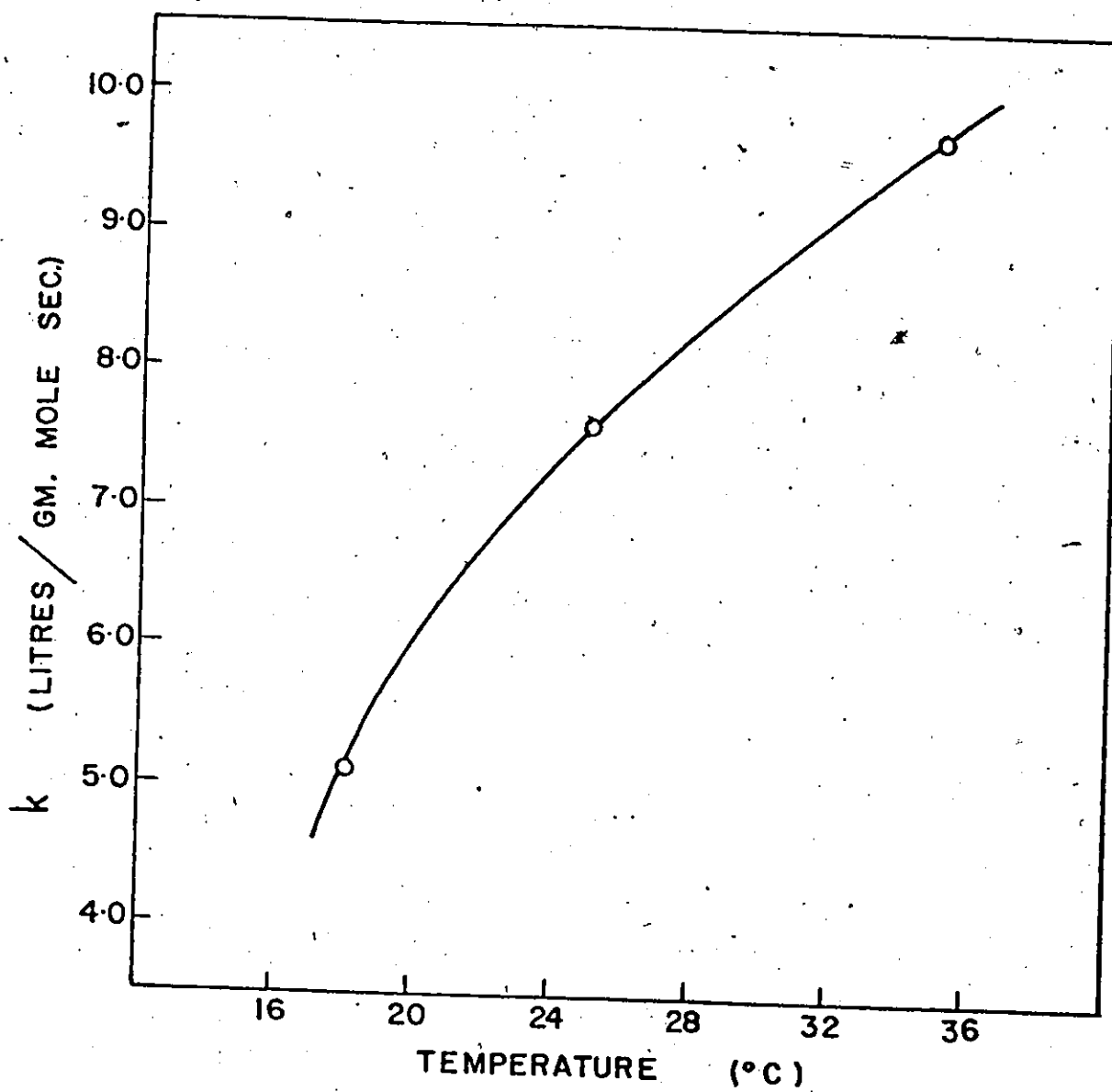


FIG. 13 . REACTION RATE CONSTANT FOR CO_2 IN AQUEOUS MEA SOLUTION AS A FUNCTION OF TEMPERATURE FROM / REF. (18)

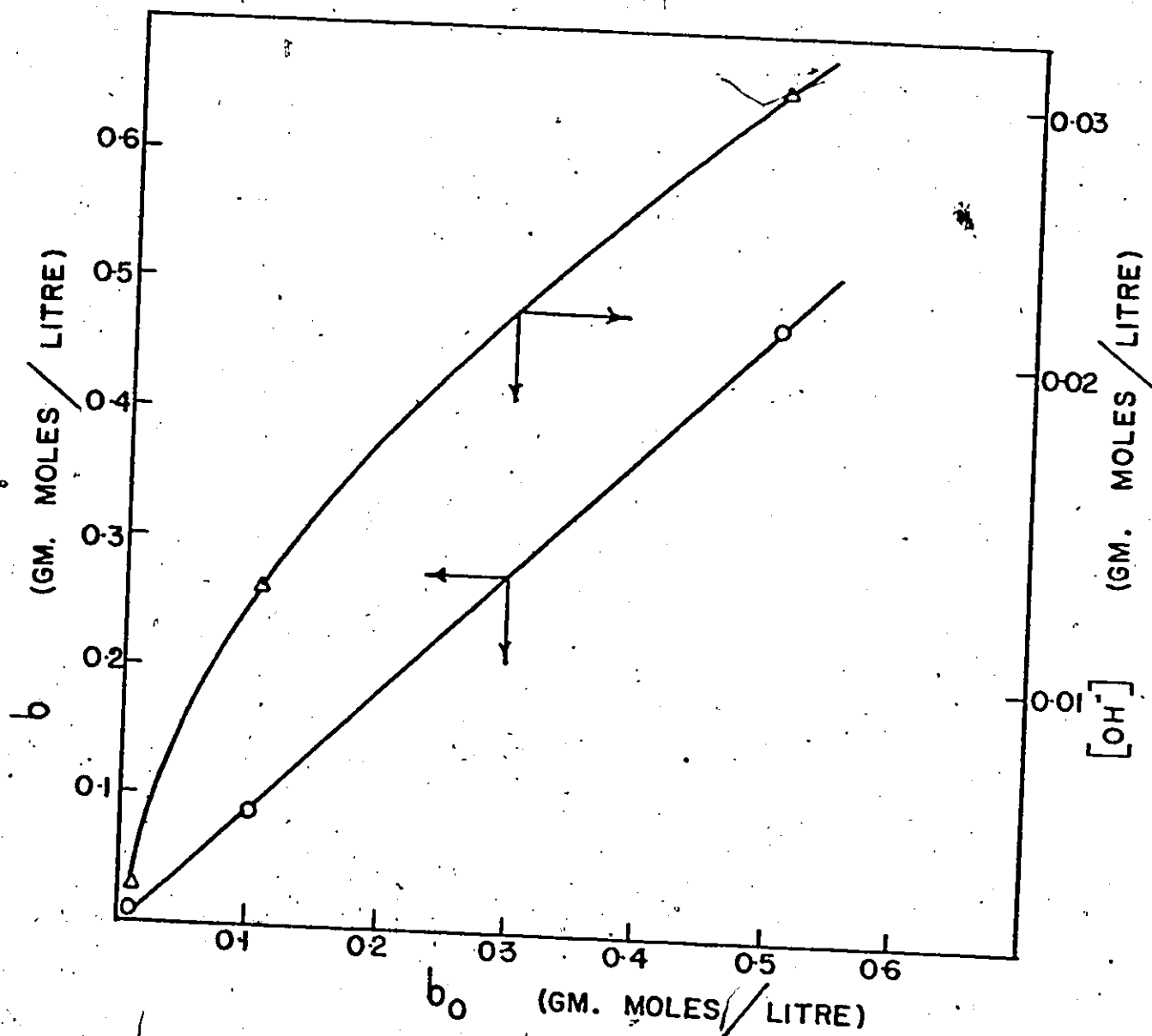


FIG. 14 IONIZATION DATA AT 25° C FOR AQUEOUS SOLUTIONS OF MEA FROM REF. (20)

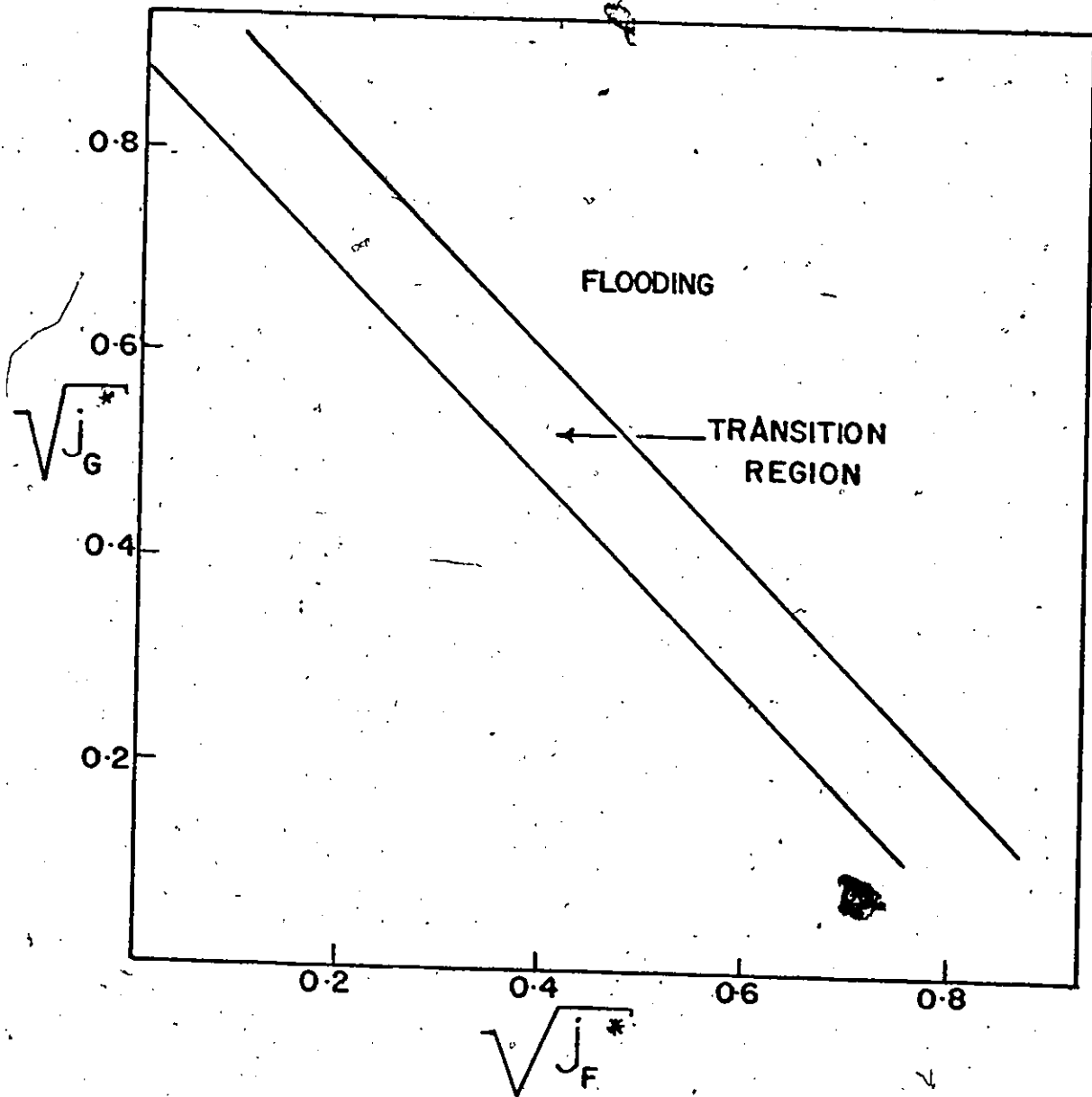


FIG. 15 FLOODING VELOCITIES FOR AIR AND WATER FROM REF. (22)

APPENDIX IV
CALIBRATION AND TITRATION CURVES

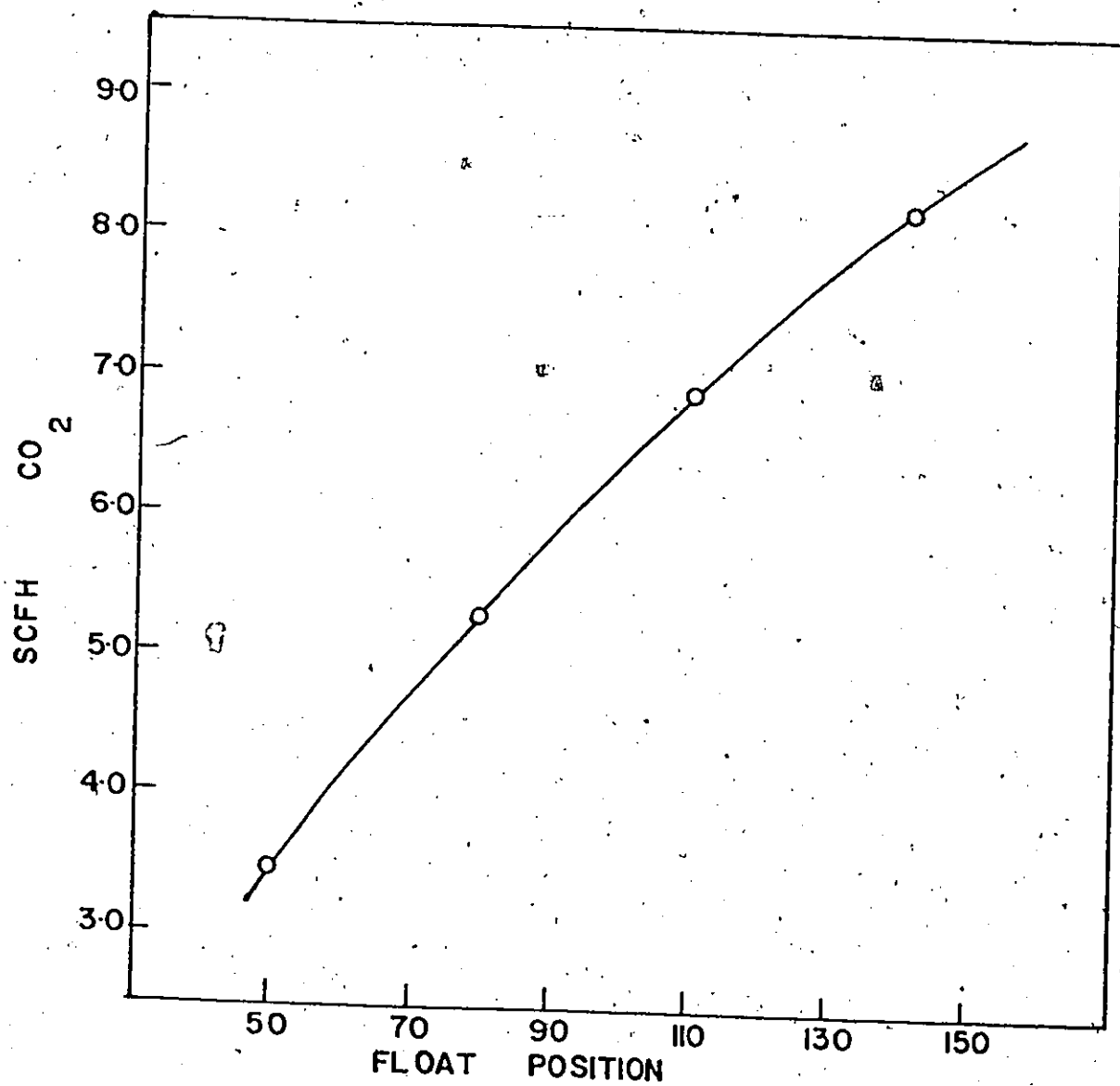


FIG. 16 CALIBRATION CURVE FOR CO₂
ROTAMETER

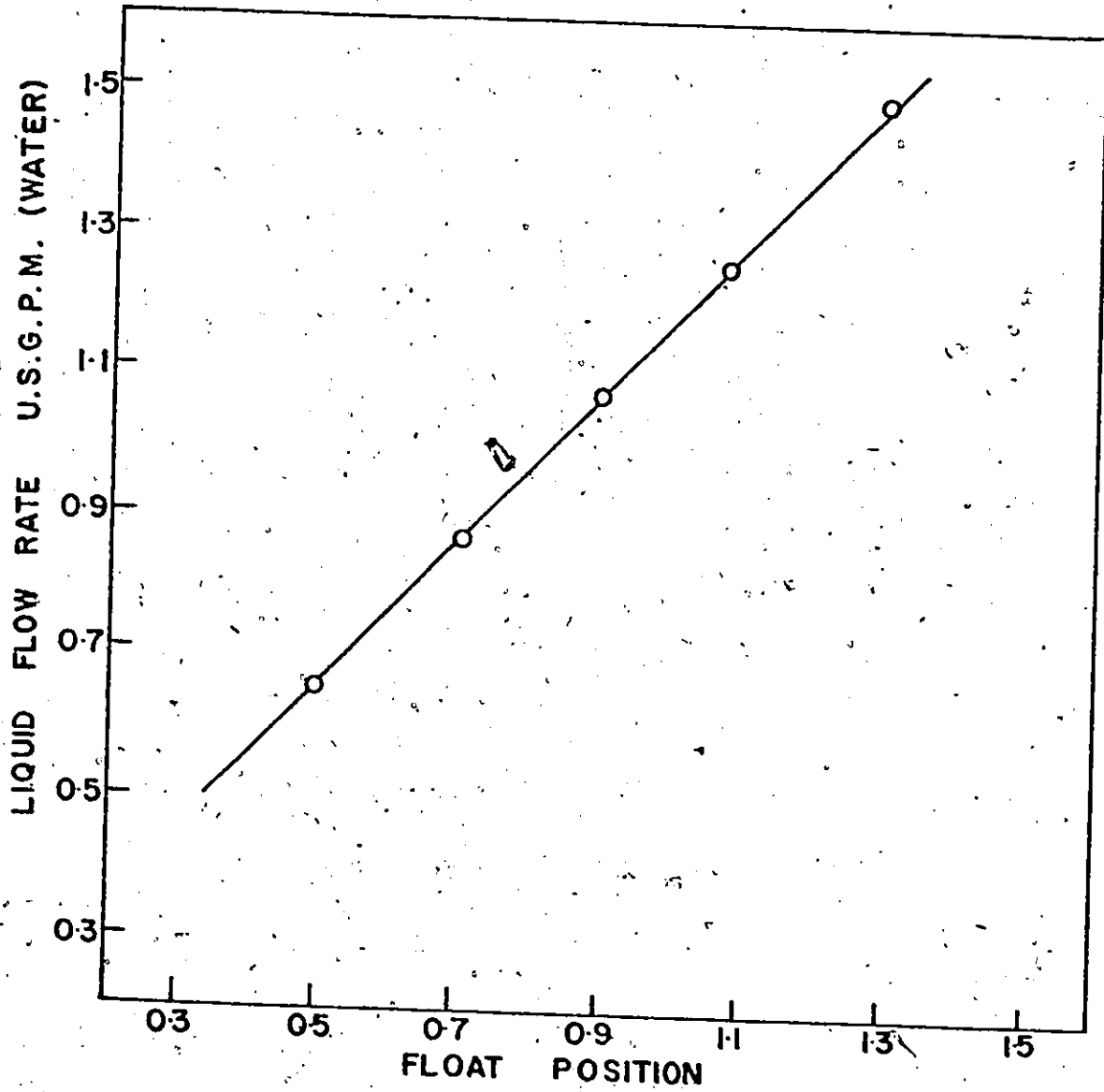


FIG. 17 CALIBRATION CURVE FOR LIQUID ROTAMETER

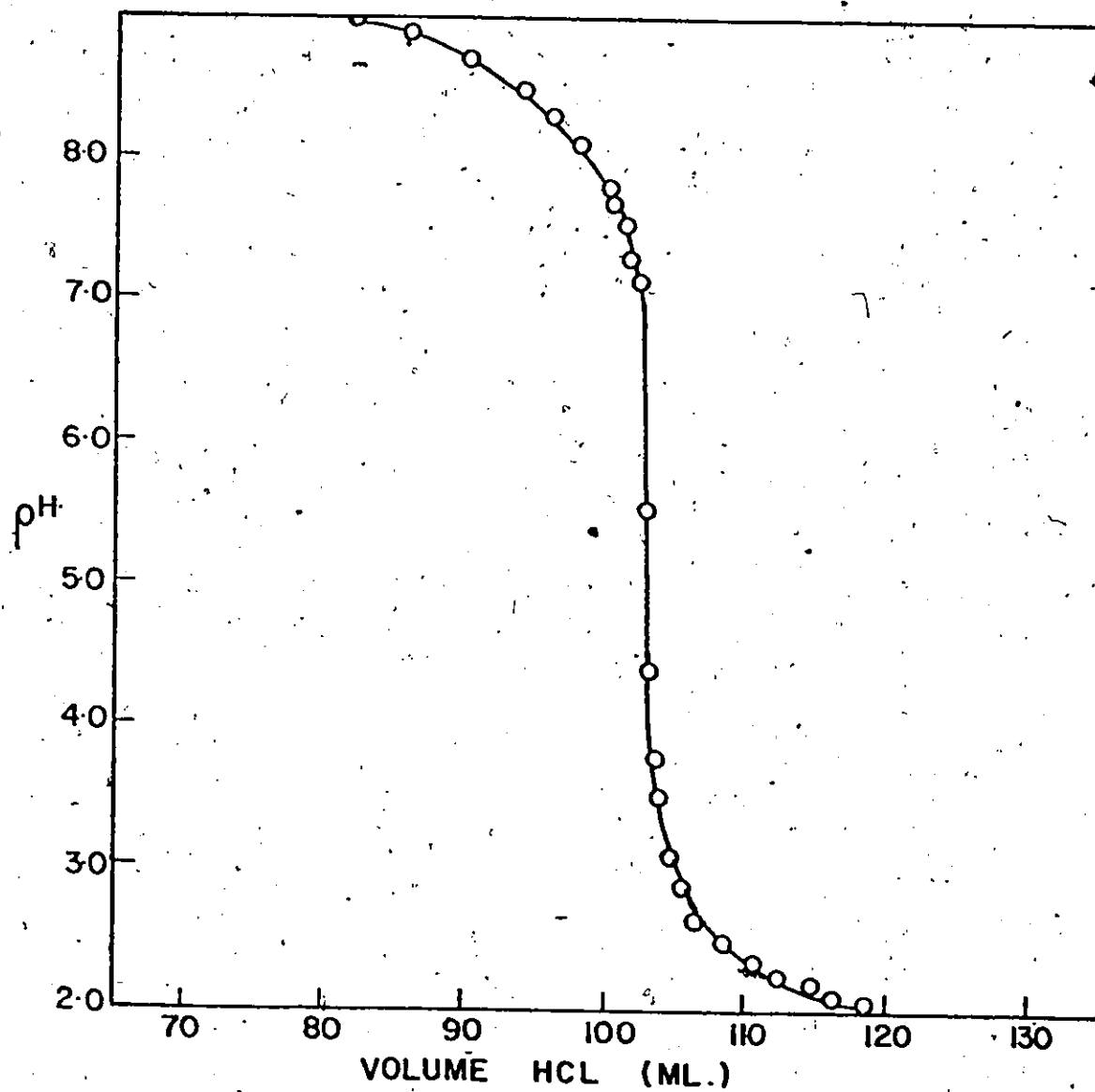


FIG. 18 TITRATION CURVE FOR 0.12 N MEA
NORMALITY HCL = 0.10

VITA AUCTORIS

- 1948 Born at Pescara, Italy on July 9.
- 1967 Admitted into the University of Windsor, Windsor, Ontario, to begin studies in the Applied Science Course.
- 1971 Received the Bachelor Degree in Chemical Engineering at Windsor, and proceeded to Graduate Studies in the same field.
- 1972 Accepted employment with Goodyear Industrial Products in Bowmanville, Ontario.